JACS
JOURNAL OF THE AMERICAN CHEMICAL SOCIETY

Article

Five- and Six-Membered Conformationally Locked 2‘,4‘-Carbocyclic *ribo*-Thymidines: Synthesis, Structure, and Biochemical Studies

Puneet Srivastava, Jharna Barman, Wimal Pathmasiri, Oleksandr Plashkevych, Magorzata Wenska, and Jyoti Chattopadhyaya

J. Am. Chem. Soc., **2007**, 129 (26), 8362-8379• DOI: 10.1021/ja071106y • Publication Date (Web): 07 June 2007

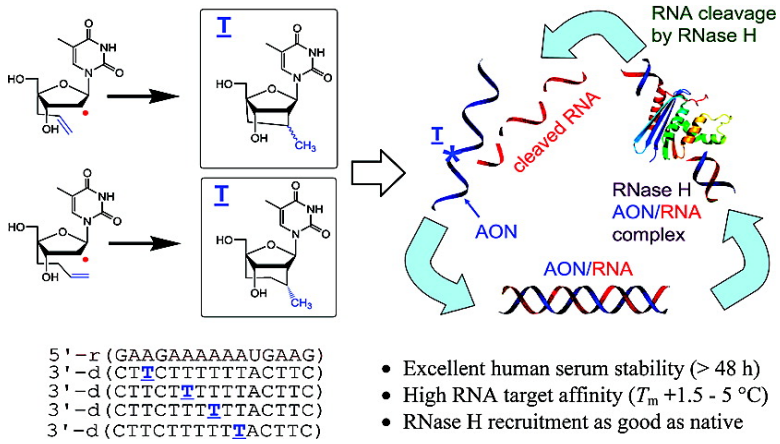

More About This Article

Additional resources and features associated with this article are available within the HTML version:

- Supporting Information
- Links to the 6 articles that cite this article, as of the time of this article download
- Access to high resolution figures
- Links to articles and content related to this article
- Copyright permission to reproduce figures and/or text from this article

View the Full Text HTML

J|A|C|S
ARTICLES
Published on Web 06/07/2007

Five- and Six-Membered Conformationally Locked 2′,4′-Carbocyclic *ribo*-Thymidines: Synthesis, Structure, and Biochemical Studies

Puneet Srivastava, Jharna Barman, Wimal Pathmasiri, Oleksandr Plashkevych, Małgorzata Wenska, and Jyoti Chattopadhyaya*

Contribution from the Department of Bioorganic Chemistry, Box 581, Biomedical Center, Uppsala University, SE-75123 Uppsala, Sweden

Received February 15, 2007; E-mail: jyoti@boc.uu.se

Abstract: Two unusual reactions involving the 5-hexenyl or the 6-heptenyl radical cyclization of a distant double bond at C4′ and the radical center at C2′ of the ribofuranose ring of thymidine have been used as key steps to synthesize North-type conformationally constrained cis-fused bicyclic five-membered and six-membered carbocyclic analogues of LNA (carbocyclic-LNA-T) and ENA (carbocyclic-ENA-T) in high yields. Their structures have been confirmed unambiguously by long range $^{1}H-^{13}C$ NMR correlation (HMBC), TOCSY, COSY, and NOE experiments. The carbocyclic-LNA-T and carbocyclic-ENA-T were subsequently incorporated into the antisense oligonucleotides (AONs) to show that they enhance the T_m of the modified AON/RNA heteroduplexes by 3.5−5 °C and 1.5 °C/modification for carbocyclic-LNA-T and carbocyclic-ENA-T, respectively. Whereas the relative RNase H cleavage rates with carbocyclic-LNA-T, carbocyclic-ENA-T, aza-ENA-T, and LNA-T modified AON/RNA duplexes were found to be very similar to that of the native counterpart, irrespective of the type and the site modification in the AON strand, a single incorporation of carbocyclic-LNA and carbocyclic-ENA into AONs leads to very much more enhanced nuclease stability in the blood serum (stable >48 h) as compared to that of the native (fully degraded <3 h) and the LNA-modified AONs (fully degraded <9 h) and aza-ENA (≈85% stable in 48 h). Clearly, remarkably enhanced lifetimes of these carbocyclic-modified AONs in the blood serum may produce the highly desired pharmacokinetic properties because of their unique stability and consequently a net reduction of the required dosage. This unique quality as well as their efficient use as the AON in the RNase H-promoted cleavage of the target RNA makes our carbocyclic-LNA and carbocyclic-ENA modifications excellent candidates as potential antisense therapeutic agents.

Introduction

Antisense[1] oligonucleotides (AON) can potentially inhibit protein synthesis by translation arrest/steric blocking or by RNase H-mediated degradation of the AON/RNA hybrid.[2] Other methods of gene silencing include formation of triplexes by base-pairing with double-helical DNA (antigene effects),[3] or RNA interference (RNAi), by a short double-stranded RNA (siRNA).[4] The *in vivo* application of the gene silencing technology warrants chemical modification of the antisense/antigene or siRNA strand to enhance the target affinity, specificity, stability in the blood serum, and tissue specific delivery in order to improve overall pharmacokinetic properties.[5] Various modifications of oligonucleotide involving sugar, phosphodiester linkage, and nucleobase are known.[6] Of these the phosphorothioate[7] backbone-modified oligonucleotides have found some use in therapeutics.[8] Recent years have seen development of conformationally constrained bicyclic (Figure 1) and tricyclic nucleotides,[9−11] in which the sugar is locked in a definite puckered conformation. Such oligonucleotides show promising properties with respect to target RNA binding and nuclease resistance.[12,13] Among several molecules reported, short nucleotides containing LNA[12] (≡BNA[14]) modifications have shown unprecedented thermal stability (+3 to +8 °C per modification depending upon the sequence context). The enhanced target binding property of the North-conformationally constrained bicyclic sugar units in these nucleotides has been

(1) Zamecnik, P. C.; Stephenson, M. L. *Proc. Natl. Acad. Sci. U.S.A.* **1978**, *75*, 280−284.
(2) Crooke, S. T. *Annu. Rev. Med.* **2004**, *55*, 61−95.
(3) Buchini, S.; Leumann, C. J. *Curr. Opin. Chem. Biol.* **2003**, *7* (6), 717−726.
(4) Montgomery, M. K.; Xu, S.; Fire, A. *Proc. Natl. Acad. Sci. U.S.A.* **1998**, *95* (26), 15502−15507.
(5) Kurreck, J. *Eur. J. Biochem.* **2003**, *270*, 1628−1644.
(6) Freier, S. M.; Altmann, K. H. *Nucleic Acids Res.* **1997**, *25*, 4429−4443.
(7) Eckstein, F. *Annu. Rev. Biochem.* **1985**, *54*, 367−402.
(8) Holmlund, J. T. *Ann. N.Y. Acad. Sci.* **2003**, *1002* (Therapeutic Oligonucleotides), 244−251.
(9) Leumann, C. J. *Bioorg. Med. Chem.* **2002**, *10*, 841−854.
(10) Steffens, R.; Leumann, C. *Helv. Chim. Acta* **1997**, *80*, 2426−2439.
(11) Wengel, J. *Acc. Chem. Res* **1999**, *32*, 301−310.
(12) Koshkin, A. A.; Singh, S. K.; Nielsen, P.; Rajwanshi, V. K.; Kumar, R.; Meldgaard, M.; Olsen, C. E.; Wengel, J. *Tetrahedron* **1998**, *54* (14), 3607−3630.
(13) Morita, K.; Takagi, M.; Hasegawa, C.; Kaneko, M.; Tsutsumi, S.; Sone, J.; Ishikawa, T.; Imanishi, T.; Koizumi, M. *Bioorg. Med. Chem.* **2003**, *11* (10), 2211−2226.
(14) Obika, S.; Nanbu, D.; Hari, Y.; Morio, K.-I.; In, Y.; Ishida, T.; Imanishi, T. *Tetrahedron Lett.* **1997**, *38* (50), 8735−8738.

10.1021/ja071106y CCC: $37.00

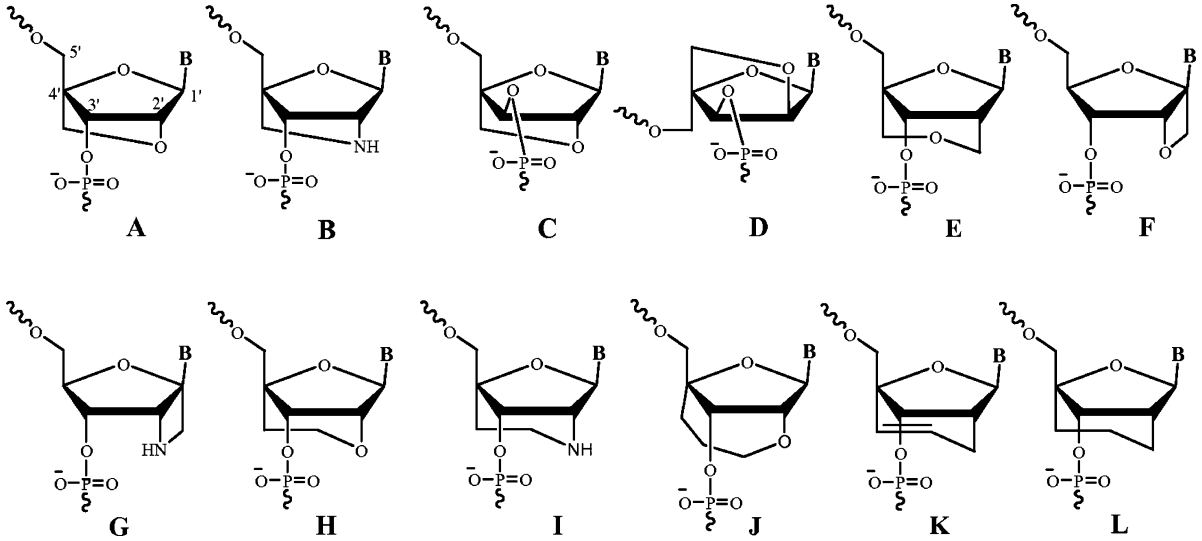

Figure 1. Structures of various bicyclic North-type conformationally constrained α/β-D/L-pentofuranosyl nucleosides: (A) LNA;[12,14] (B) amino-LNA;[16] (C) xylo-LNA;[21] (D) α-L-LNA;[22] (E) β-bicyclonucleoside;[23] (F) 1′,2′-oxetane-bridged;[17] (G) 1′,2′-azetidine-bridged;[18] (H) ENA;[13,24−26] (I) aza-ENA;[20] (J) PrNA;[13] (K) unsaturated carbocyclic analogue of LNA;[27] (L) saturated carbocyclic analogue of LNA.[27]

attributed to the improved stacking between the nearest neighbors and quenching of concerted local backbone motions by LNA nucleotides in ssLNA so as to reduce the entropic penalty in the free energy of stabilization for the duplex formation with RNA.[15] These bicyclic constrained analogues have thus been extensively used to facilitate the down-regulation of genes.[5] The features of LNA/BNA have led to the synthesis of a number of closely related analogues, in which the 2′,4′-bridge has been altered[16] or a new type of 1′,2′-bridged constraint has been introduced, such as in the 1′,2′-oxetane[17] or 1′,2′-azetidine[18] analogue. Such modifications show similar or moderately depressed T_m properties when compared to LNA, but the nuclease resistance or RNase H recruitment properties (for example, ENA,[19] PrNA,[13] and aza-ENA[20]) have turned out to be relatively more favorable than those exhibited by the LNA-containing AONs.

Studies[28] with modified nucleotides show that substituents play an important role in conformational steering, controlling hydration, inducing hydrophobic/hydrophilic interactions, and generally using the electrostatic interactions[29] to neutralize, for example, the phosphates charge, as well as to influence interaction of modified oligonucleotides with other nucleotides and/or enzymes present in the system.[30] We and others[31,32] have argued that replacement of the hydrophilic 2′-oxygen of LNA[12] or ENA[19] or 2′-nitrogen from their amino analogues[16] by the hydrophobic carbocyclic analogues would steer both target affinity as well as the nuclease stability in the blood serum because of change in the immediate shell of hydration. Recently,[27] the ring-closing metathesis approach had been employed to synthesize two carbocyclic analogues of ENA with three carbons locking the C2′ and C4′ (compounds K/L in Figure 1). These carbocyclic analogues had been incorporated into AONs with a natural phosphodiester backbone which leads to increased thermal stability (T_m) by 2.5−4.5 °C/modification with the complementary RNA. However, no blood serum or 3′-exonuclease stability or RNase H recruitment capability of these carbocyclic analogues has so far been reported.

Here we report a novel synthetic strategy for the carbocyclic analogues of LNA[12] and ENA[13] thymidines (carbocyclic-LNA-T and carbocyclic-ENA-T), which have been accomplished using an intramolecular free-radical ring-closure reaction between a radical generated at C2′ and a strategically placed double bond in the modified pentofuranose moiety of the nucleoside. We have subsequently incorporated carbocyclic-LNA-T [$T_{(5-carbo)}$]and carbocyclic-ENA-T [with $T_{(6-carbo)}$] into the AONs and studied their blood serum stabilities, as well as their RNase H recruitment capabilities, and compared these properties with isosequential LNA[12,14]- and aza-ENA[20]-containing counterparts.

Results and Discussion

The intramolecular radical addition reactions to the tethered double bond involving both 5-hexenyl and 6-heptenyl radicals[33]

(15) Petersen, M.; Nielsen, C. B.; Nielsen, K. E.; Jensen, G. A.; Bondensgaard, K.; Singh, S. K.; Rajwanshi, V. K.; Koshkin, A. A.; Dahl, B. M.; Wengel, J.; Jacobsen, J. P. *J. Mol. Recognit.* **2000**, *13* (1), 44−53.
(16) Singh, S. K.; Kumar, R.; Wengel, J. *J. Org. Chem.* **1998**, *63* (26), 10035−10039.
(17) Pradeepkumar, P. I.; Cheruku, P.; Plashkevych, O.; Acharya, P.; Gohil, S.; Chattopadhyaya, J. *J. Am. Chem. Soc.* **2004**, *126*, 11484−11499.
(18) Honcharenko, D.; Varghese, O. P.; Plashkevych, O.; Barman, J.; Chattopadhyaya, J. *J. Org. Chem.* **2006**, *71*, 299−314.
(19) Koizumi, M. *Curr. Opin. Mol. Ther.* **2006**, *8*, 144−149.
(20) Varghese, O. P.; Barman, J.; Pathmasiri, W.; Plashkevych, O.; Honcharenko, D.; Chattopadhyaya, J. *J. Am. Chem. Soc.* **2006**, *128* (47), 15173−15187.
(21) Babu, B. R.; Raunak; Poopeiko, N. E.; Juhl, M.; Bond, A. D.; Parmar, V. S.; Wengel, J. *Eur. J. Org. Chem.* **2005**, *11*, 2297−2321.
(22) Rajwanshi, V. K.; Hakansson, A. E.; Sorensen, M. D.; Pitsch, S.; Singh, S. K.; Kumar, R.; Nielsen, P.; Wengel, J. *Angew. Chem., Int. Ed.* **2000**, *39* (9), 1656−1659.
(23) Wang, G.; Giradet, J. L.; Gunic, E. *Tetrahedron* **1999**, *55*, 7707−7724.
(24) Morita, K.; Hasegawa, C.; Kaneko, M.; Tsutsumi, S.; Sone, J.; Ishikawa, T.; Imanishi, T.; Koizumi, M. *Bioorg. Med. Chem. Lett.* **2001**, *12* (1), 73−76.
(25) Morita, K.; Yamate, K.; Kurakata, S.; Abe, K.; Imanishi, T.; Koizumi, M. *Nucleic Acids Res. Sup.* **2002**, *2*, 99−100.
(26) Morita, K.; Yamate, K.; Kurakata, S.-I.; Watanabe, K.; Imanishi, T.; Koizumi, M. *Nucleosides, Nucleotides Nucleic Acids* **2003**, *22*, 1619−1621.
(27) Albaek, N.; Petersen, M.; Nielsen, P. *J. Org. Chem.* **2006**, *71* (20), 7731−7740.
(28) Teplova, M.; Minasov, G.; Tereshko, V.; Inamati, G. B.; Cook, P. D.; Manoharan, M.; Egli, M. *Nat. Struct. Mol. Biol.* **1999**, *6* (6), 535−539.
(29) Prakash, T. P.; Pueschl, A. P.; Lesnik, E.; Mohan, V.; Tereshko, V.; Egli, M.; Manoharan, M. *Org. Lett.* **2004**, *6* (12), 1971−1974.
(30) Kanazaki, M.; Ueno, Y.; Shuto, S.; Matsuda, A. *J. Am. Chem. Soc.* **2000**, *122* (11), 2422−2432.
(31) Monia, B. P.; Johnston, J. F.; Sasmor, H.; Cummins, L. L. *J. Biol. Chem.* **1996**, *271* (24), 14533−14540.
(32) Prhavc, M.; Prakash, T. P.; Minasov, G.; Cook, P. D.; Egli, M.; Manoharan, M. *Org. Lett.* **2003**, *5* (12), 2017−2020.

have been well studied by Beckwith,[34,35] Baldwin,[36−38] Giese,[39] Curran,[40,41] Stork,[42] and more recently by Rajanbabu.[43−46] The efficiency and regiochemistry[47] of such intramolecular cyclization addition reactions have been shown to be controlled by (i) the initial radical structure, (ii) the steric effects resulting from the olefin substitution pattern,[34] and (iii) the geometric constraints on the chain linking the radical center, and the tethered double bond.[47]

In the kinetically controlled rearrangement of variously substituted 5-hexenyl radicals, the preference for the exo versus endo mode, i.e., the formation of the five-membered over the six-membered ring, is well understood in terms of a relatively strain-free chairlike transition state[47] accommodating the stereoelectronic requirements of radical addition to the double bond. The model also provides satisfactory explanation for the observed stereoselectivities in the cyclization of 2-, 3-, and 4-substituted hexenyl radicals (5-hexenyl nomenclature[48]) on account of the preferred adoption of pseudo-equatorial positions by the substituents in the respective transition states.[45]

It is known[43] that the ring-closure reaction involving cyclic 5-hexenyl radicals (i.e., radical as a part of the cyclic ring) is similar to that of the open-chain systems except that the ring imposes steric constraints on the stereochemical outcome of the reaction. The initial radical forms the most stable structure with bulky substituents in the equatorial/pseudo-equatorial position,[45] when the radical center is a part of the sugar ring. Ring-closure reaction occurs via attack of a radical center oriented to the pseudo-equatorial position on the axially substituted alkenyl chain resulting in the cis-fused rings.[35] It is also known that the alkenyl chain preferentially occupies an axial position, since an equatorial alkenyl chain results in poor overlap of the semioccupied molecular orbitals and π^* orbitals.[35]

The substituents play their role on account of their steric bulk or stereoelectronic nature as they interact with the ring atoms/substituents at different positions of alkenyl chain during intramolecular 5-hexenyl cyclization.[49] For example, it has been shown that substituents on the C1 and C4 atoms (5-hexenyl nomenclature[48]) of the initial radical are the major factors dictating stereochemistry of the newly formed 1,5-bond. Thus when both C1 and C4 substituents are present, predominantly a 1,5-cis isomer is formed.[44] With no substitution at C4 (i.e., C4-deoxy), a mixture of 1,5-cis and 1,5-trans-fused products is formed. In the presence of vinylic oxygen the boatlike transition state is stabilized resulting in formation of 1,5-trans isomer.[46]

In contradistinction, the formation of six-membered rings by free radical reactions involving 6-exo cyclizations of heptenyl system presents at least two problems: first, the rate constant of 6-hepetenyl cyclization is ≈40 times slower than the corresponding 5-hexenyl cyclization; thus, the competing radical quenching by reduction with nBu$_3$SnH becomes a serious problem. Second, the endo mode of cyclization is only ≈7 times less rapid than the exo mode of cyclization; thus, formation of the endo products also competes with the six-membered products.[48] Thus far, most of the fused bicyclic ring formation reactions studied have been of 1,2-type,[51−58] i.e., the radical center is located at the neighboring carbon to the tethered double bond.

Here we present two unusual reactions involving the 5-hexenyl or the 6-heptenyl radical cyclization by forming a C−C bond from a distant double bond at C4′ toward the C2′ radical center of the ribofuranose ring of thymidine (Scheme 1). The 2′,4′-free-radical cyclization is a key step in our synthetic strategy to efficiently yield North-type conformationally constrained cis-fused bicyclic five-membered and six-membered carbocyclic analogues of LNA (carbocyclic-LNA-T) and ENA (carbocyclic-ENA-T), as it has been originally used in the construction of conformationally constrained nucleosides by Wengel's[12] and Imanishi's[14] group in the ionic ring-closure reaction. To the best of our knowledge the only other similar case of radical cyclization reported had involved a tethered double bond (butenyl side chain) and a cyclic radical (Figure 2) in the constrained norbornyl system.[50] The double-bond chain and the free radical in the norbornyl system were positioned at C1 and C3 to each other with the stereochemistry being dictated by topological and steric constraints with four asymmetric centers, giving the 1,6-cis-fused (37%) and 1,6-trans-fused (25%) cyclohexyl ring through the participation of presumably chairlike 6-heptenyl cyclization. Clearly, in our case (Figure 3) the site of the propenyl or the butenyl substituent at C4′ with respect to the radical center at C2′ in the flexible five-membered pentofuranose ring[59] led us to assume that our free-radical cyclization reaction may have poorer steric and stereoelectronic control on the formation of a chairlike or/and boatlike transition state to give the 1,3-cis-fused ring-closure product(s).

1.0. Synthesis of the Carbocyclic-LNA-T Phosphoramidite (14). The synthesis starts from a known sugar precursor **1**[12] which was selectively benzylated using a reported procedure[20] to give the corresponding benzylated product **2**. The primary alcohol in sugar **2** was oxidized to the corresponding aldehyde

(33) Hanessian, S.; Dhanoa, D. S.; Beaulieu, P. L. *Can. J. Chem.* **1987**, *65* (8), 1859−1866.
(34) Beckwith, A. L. J. *Tetrahedron* **1981**, *37* (18), 3073−3100.
(35) Beckwith, A. L. J.; Phillipou, G.; Serelis, A. K. *Tetrahedron Lett.* **1981**, *29*, 2811−2814.
(36) Baldwin, J. E. *J. Chem. Soc. Chem. Commun.* **1976**, *18*, 738−741.
(37) Baldwin, J. E. *J. Chem. Soc. Chem. Commun.* **1976**, *18*, 734−736.
(38) Baldwin, J. E.; Cutting, J.; Dupont, W.; Kruse, L.; Silberman, L.; Thomas, R. C. *J. Chem. Soc. Chem. Commun.* **1976**, *18*, 736−738.
(39) Giese, B. *Angew. Chem.* **1983**, *95* (10), 771−782.
(40) Curran, D. P. *Synthesis* **1988**, *6*, 417−439.
(41) Curran, D. P. *Synthesis* **1988**, *7*, 489−513.
(42) Stork, G.; Baine, N. H. *J. Am. Chem. Soc.* **1982**, *104* (8), 2321−2323.
(43) RajanBabu, T. V. *J. Org. Chem.* **1988**, *53* (19), 4522−4530.
(44) RajanBabu, T. V. *Acc. Chem. Res.* **1991**, *24* (5), 139−145.
(45) RajanBabu, T. V.; Fukunaga, T. *J. Am. Chem. Soc.* **1989**, *111* (1), 296−300.
(46) RajanBabu, T. V.; Fukunaga, T.; Reddy, G. S. *J. Am. Chem. Soc.* **1989**, *111* (5), 1759−1769.
(47) Beckwith, A. L. J.; Schiesser, C. H. *Tetrahedron* **1985**, *41* (19), 3925−3941.
(48) Motherwell, W. B.; Crich, D. *Free radical chain reactions in organic synthesis*; Academic Press: New York, 1992, 0-12-508760-8.
(49) Beckwith, A. L. J.; Page, D. M. *Tetrahedron* **1999**, *55* (11), 3245−3254.
(50) Bakuzis, P.; Campos, O. O. S.; Bakuzis, M. L. F. *J. Org. Chem.* **1976**, *41* (20), 3261−3264.
(51) Lopez, J. C.; Fraser-Reid, B. *J. Am. Chem. Soc.* **1989**, *111* (9), 3450−3452.
(52) Lopez, J. C.; Gomez, A. M.; Fraser-Reid, B. *J. Chem. Soc. Chem. Commun.* **1993**, *9*, 762−764.
(53) Lopez, J. C.; Gomez, A. M.; Fraser-Reid, B. *J. Chem. Soc. Chem. Commun.* **1994**, *13*, 1533−1534.
(54) Lopez, J. C.; Gomez, A. M.; Fraser-Reid, B. *J. Org. Chem.* **1995**, *60* (12), 3871−3878.
(55) Xi, Z.; Agback, P.; Plavec, J.; Sandstroem, A.; Chattopadhyaya, J. *Tetrahedron* **1992**, *48* (2), 349−370.
(56) Xi, Z.; Agback, P.; Sandstroem, A.; Chattopadhyaya, J. *Tetrahedron* **1991**, *47* (46), 9675−9690.
(57) Xi, Z.; Glemarec, C.; Chattopadhyaya, J. *Tetrahedron* **1993**, *49* (34), 7525−7546.
(58) Xi, Z.; Rong, J.; Chattopadhyaya, J. *Tetrahedron* **1994**, *50* (17), 5255−5272.
(59) Thibaudeau, C.; Acharya, P.; Chattopadhyaya, J. *Stereoelectronic Effects in Nucleosides & Nucleotides and their Structural Implications*; Uppsala University Press: Uppsala, 1999, 91-506-1351-0.

Scheme 1 [a]

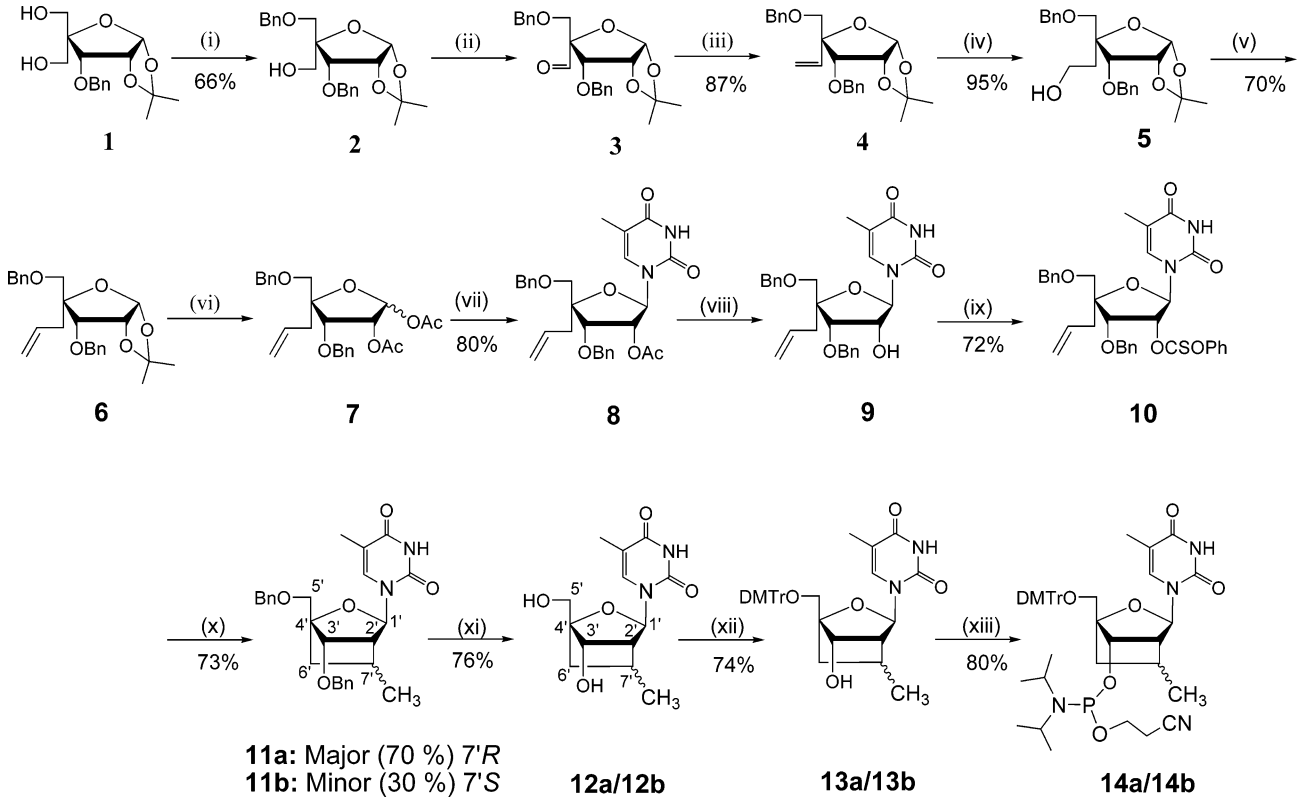

[a] Reagents and conditions: (i) NaH, BnBr, −5 °C to rt overnight; (ii) oxalyl chloride, DMSO, −78 °C, DIPEA, DCM; (iii) $PPh_3{}^+CH_3Br^-$, 1.6 M butyllithium in hexane, THF, −78 °C to rt overnight; (iv) 9-BBN, THF, 3 N NaOH, 33% H_2O_2; (v) oxalyl chloride, DMSO, −78 °C, DIPEA, DCM, $PPh_3{}^+CH_3Br^-$, 1.6 M butyllithium in hexane, THF, −78 °C to rt overnight; (vi) acetic acid, acetic anhydride, triflic acid; (vii) persilylated thymine, TMSOTf, CH_3CN, 0 °C to rt overnight; (viii) 27% methanolic NH_3, overnight; (ix) DMAP, phenyl chlorothionoformate, pyridine; (x) Bu_3SnH, toluene, AIBN, 4 h; (xi) 20% $Pd(OH)_2$/C, Ammonium Formate, Methanol, Reflux, 8 h; (xii) DMTr-Cl, Pyridine, Overnight; (xiii) 2-cyanoethyl *N*,*N*-diisopropylphosphoramidochloridite, DIPEA, dry THF, overnight. The IUPAC numbering according to von Bayer nomenclature for bicyclic systems is used in the Experimental Section. Abbreviations: Bn (benzyl); Ac (acetyl); 9-BBN (9-borobicyclo(3.3.1)nonane); THF (tetrahydrofuran); AIBN, [2,2′-azobis(2-methyl-propionitrile)]; DMTr (4,4′-dimethoxytrityl; DIPEA, diisopropylethylamine).

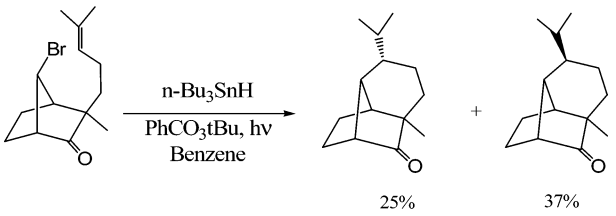

Figure 2. Heptenyl cyclization of 7-norborneyl radical.[50]

3 employing Swern oxidation.[60] The vinyl chain at C4 was then introduced by the Wittig reaction[61] on the crude aldehyde **3** to give the vinyl sugar **4** (87% in two steps from **2**). The olefin **4** was converted to the C4-hydroxyethyl derivative via successive hydroboration−oxidation using 9-BBN/NaOH−H_2O_2 to give **5** in 95% yield, which was again subjected to Swern oxidation[60]/Wittig[61] reaction to give the required C4-allylated sugar **6** (70% in two steps from **5**) with a strategically placed propenyl side chain at C4 for 5-hexenyl type free radical cyclization. Compound **6** was subjected to acetolysis using a mixture of acetic anhydride, acetic acid, and triflic acid to give the corresponding diacetate **7** quantitatively as an α/β anomeric mixture (single spot on TLC and proven by ^{1}H NMR). The crude diacetate **7**, after bicarbonate workup, was subjected to a modified Vorbruggen reaction[62] involving *in situ* silylation of thymine and subsequent trimethylsilyl triflate-mediated coupling to give thymine nucleoside **8** in 80% yield in two steps from **6**. The β-configuration of the product **6** was confirmed by a 1D differential NOE experiment, which showed 3% enhancement of H2′ and a 1% enhancement of H3′ upon irradiation of H6 ($d_{H6-2'} \approx 2.3$ Å for β anomer). Deacetylation of compound **8** using 27% methanolic ammonia overnight and subsequent esterification using phenyl chlorothioformate yielded the desired precursor **10** for radical cyclization. The key free-radical cyclization reaction was carried out using Bu_3SnH with radical initiator AIBN at 115 °C in degassed (N_2) toluene. To ensure that the radical generated has an adequate lifetime to capture the double bond before it is quenched by a hydrogen radical, the concentrations of Bu_3SnH and AIBN were maintained through high dilution and slow dropwise addition. The 5-hexenyl type exo mode cyclization of the radical to the C4′-propenyl double bond yielded exclusively the expected[34] five-membered 2′,4′-cis-fused carbocyclic product with a bicyclo[2.2.1]heptane skeleton as an inseparable diastereomeric mixture of compounds **11a** (major compound 70%, 7′*R*) and **11b** (minor compound 30%, 7′*S*).

The formation of the bicyclic nucleosides **11a** and **11b**, with a North-fused conformationally constrained pentofuranosyl

(60) Mancuso, A. J.; Brownfain, D. S.; Swern, D. *J. Org. Chem.* **1979**, *44* (23), 4148−4150.
(61) Wittig, G.; Schlosser, M. *Angew. Chem.* **1960**, *72*, 324.
(62) Vorbrüggen, H.; Höfle, G. *Chem. Ber* **1981**, *114*, 1256−1258.

Scheme 2 [a]

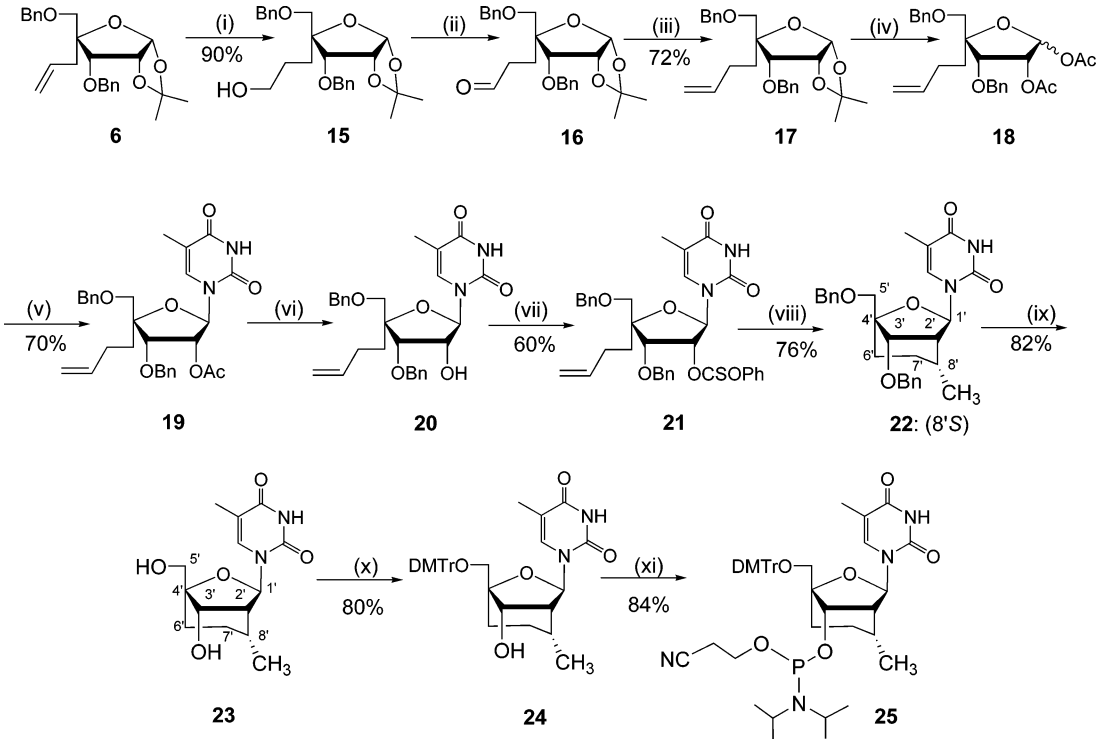

[a] Reagents and conditions: (i) 9-BBN, THF, overnight, 3 M NaOH, 33% H_2O_2; (ii) oxalyl chloride, DMSO, −78 °C, DIPEA, CH_2Cl_2; (iii) $PPh_3{}^+CH_3Br^-$, THF, 1.6 M butyllithium in hexane, −78 °C to rt overnight; (iv) acetic acid, acetic anhydride, triflic acid; (v) persilylated thymine, TMSOTf, CH_3CN, 0 °C to rt overnight; (vi) 27% methanolic NH_3, overnight; (vii) DMAP, phenyl chlorothionoformate, pyridine, rt overnight; (viii) Bu_3SnH, toluene, AIBN, 4 h, reflux; (ix) 20% Pd(OH), ammonium formate, methanol, reflux,12 h; (x) DMTr-Cl, pyridine, rt overnight; (xi) 2-cynoethyl *N*,*N*-diisopropylphosphoramidochloridite, DIPEA, dry THF. The IUPAC numbering according to von Bayer nomenclature for bicyclic systems is used in the Experimental Section. Abbreviations: Bn (benzyl); Ac (acetyl); 9-BBN (9 borobicyclo(3.3.1)nonane); THF (tetrahydrofuran); AIBN, [2,2′-azobis(2-methyl-propionitrile)]; DMTr (4,4′-dimethoxytrityl); DIPEA (diisopropylethylamine).

moiety, was confirmed by long range $^1H-^{13}C$ NMR correlation (HMBC)[63] and $^1H-^1H$ (TOCSY)[64] for both the isomers (see Section 4). A 1D differential NOE experiment (Figure 5) established that the exocyclic methyl at C7′ is in close proximity to H1′ in the major isomer ($d_{7'-Me/H1'} = 2.8$ Å for *R* and 4.4 Å for *S*-configuration at C7′) of the bicyclic structure. The benzyl groups in the bicyclic nucleosides **11a/11b** were deprotected using $Pd(OH)_2/C$ and ammonium formate in methanol to give the corresponding dihydroxy compounds **12a** and **12b**, respectively (see Section 4). Several attempts to separate this diastereomeric mixture of **12a/12b** failed in our hands. We therefore subjected it directly to 5′-dimethoxytritylation (74%) to give **13** followed by 3′-phosphitylation (80%) to give the phosphoramidite **14** using standard conditions.[18]

2.0. Synthesis of Carbocyclic-ENA-T Phosphoramidite (25). For the synthesis of carbocyclic-ENA-T analogue, a heptenyl type of free-radical intermediate was warranted, and thus the C4-allylated sugar **6** obtained in the previous scheme was subjected to another round of hydroboration−oxidation followed by Swern oxidation[60] and Wittig[61] reaction, as for **4**, **5**, and **6** in Scheme 1, to yield **15** (90%), **16** and **17** (72% in two steps), respectively (Scheme 2). The sugar **17** was subjected to acetolysis followed by a modified Vorbruggen-type[62] coupling, as for compounds **7** and **8** in Scheme 1, to give **18** and *β*-configured thymine nucleoside **19** in 70% yield in two steps. Deacetylation with 27% methanolic ammonia followed by esterification using phenyl chlorothioformate yielded the ester **21** (60% yield). Purified ester was then subjected to free-radical cyclization utilizing tributyltin hydride in the presence of radical initiator AIBN. Though for the heptenyl type of cyclization the endo mode is only 7 times less rapid than the exo mode cyclization in addition to the competing 1,5-hydrogen abstraction,[48] the reaction gave, however, exclusively exo-product **22** in modest 76% yield. The bicyclic nucleoside **22** was deprotected using $Pd(OH)_2/C$ and ammonium formate in methanol to give the corresponding dihydroxy compound **23** with 6-oxabicyclo[3.2.1]octane in 82% yield. Dimethoxytritylation (80%) followed by phosphitylation using standard conditions[20] gave the fully protected phosphoramidite **25** in 84% yield.

3.0. Mechanism of the Ring-Closure Reaction. Two possible transition states TS **1** and TS **2** could be involved in the radical cyclization of the C4′-propenyl system through the 5-*exo*-hexenyl intermediate (structure **A** in Figure 3) in which case these transition states should represent the low-energy chair forms with a newly developing C7′ methyl substituent in the pseudo-equatorial (TS **1**) or pseudoaxial (TS **2**) orientation. Although both transition states are probable, the experimental evidence (7:3 proportion of major to minor products) suggests that the absence of 1,3-diaxial interactions of the methyl group at C7′ (C7′ in *R*-configuration) with the bulky protective Bn group at the pseudoaxial O3′ (**11a**) is energetically more favorable and the product with methyl group at C7′ in *S*-configuration (**11b**) is the minor product. We anticipate that the energy of stabilization of the transition state TS **1** is slightly

(63) Bax, A.; Summers, M. *J. Am. Chem. Soc.* **1986**, *108*, 2093−2094.
(64) Bax, A.; Davis, D. G. *J. Magn. Reson.* **1985**, *65*, 355−360.

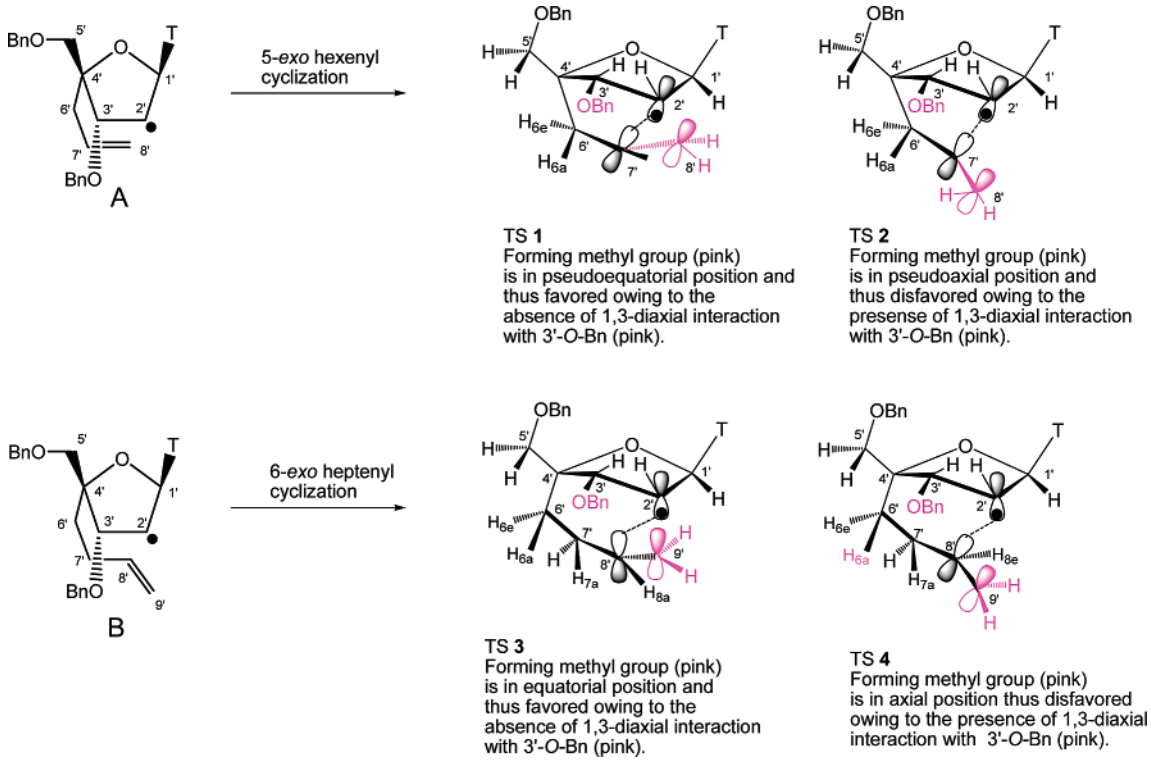

Figure 3. **(**A**)** 5-Exo-cyclization through two transition states TS **1** and TS **2** leading to favored five-membered carbocyclic 2′,4′-cis-fused bicyclic system with *R*-configuration of C7′ chiral center as well as to the counterpart with the disfavored *S*-configuration of C7′. **(**B**)** 6-*exo*-Heptenyl cyclization through two transition states TS **3** and TS **4** leading to favored carbocyclic 2′,4′-cis-fused bicyclic system with *R*-configuration of C8′ and its counterpart with C8′ chiral center in the disfavored *S*-configuration.

more because of the absence of any nonbonding/steric interaction compared to that in the TS **2**.

Similar considerations can be used to understand the mechanism of the 6-*exo*-heptenyl cyclization of substituted nucleoside radical **B** (Figure 3). For cyclization to occur, two favorable (out of four possible) configurations obtained by rotation around C6′−C7′ in the side chain, C4′−C6′−C7′−C8′, and around C7′−C8′ in the C6′−C7′−C8′−C9′, represent probable transition states TS **3** and TS **4**. The position of C7′−C8′ double bound is apparently in a close proximity of the forming radical at C2′ which makes the cyclic product arising from the TS **3** transition state (Figure 3) a preferable reaction path. The newly developing C8′ methyl substituent thus takes up the equatorial position, in which the 1,3-diaxial interaction with the C3′ axial substituent (OBn) in the newly formed fused cyclohexyl ring is absent, which makes it more favored then the product with chiral C8′ in *S*-configuration.

The orientation of the transition state, TS **4** in Figure 3, on the other hand, is also in a chair conformation, with site of attack in the double bond (C8′) and the radical center at C3′ in the steric proximity in order to ensure 6-*exo*-heptenyl cyclization with minimal entropic penalty. This orientation in TS **4**, however, exhibits two 1,3-diaxial interactions, one between the 3′-*O*-benzyl substituent and the newly developing axial methyl substituent at C8′ and, second, between the newly forming C8′ methyl substituent and the axial proton at C6′. The presence of two 1,3-diaxial interactions would result in a energetically disfavored transition state, as shown in TS **4**, compared to that in TS **3**, which explains why we observe the exclusive formation of the cyclic product with equatorial methyl at C8′ (Figure 3).

4.0. Assignment of ^{1}H and ^{13}C Chemical Shifts and Evidence for the Ring Closure in the Five-Membered Fused Carbocyclic-LNA-T (12a and 12b) and the Six-Membered Carbocyclic-ENA-T (23). The ^{1}H spectrum at 600 MHz of the ring-closure reaction of the parent olefin **10** revealed that the product formed is an intractable diastereomeric mixture of the sugar-fused five-membered bicyclic 3′,5′-di-*O*-benzyl protected nucleosides **11a/11b** (Scheme 1). However, because of the overlap of the H7′ and H2′ peaks in **11a/11b**, firm NMR evidence could not be obtained for the carbon−carbon ring closure between C2′ and C7′. It is noteworthy that the high-resolution mass spectrometry would not be able to discriminate between the mass of the 2′-deoxy counterpart of **10** (formed as a result of 2′-deoxygenation and subsequent quenching by a hydrogen radical)[65] and the cyclized product **11a/11b**. The H7′ and H2′ peaks in the deprotected compounds **12a/12b** were however fully resolved and hence could be successfully used for full NMR characterization.

The ^{1}H spectrum (Figure S22 in Supporting Information (SI)) showed the presence of two diastereomers, a major (**12a**) as well as a minor isomer (**12b)** in *ca*. 7:3 ratio. The upfield H2′ at δ 2.43 along with H7′ at δ 2.65 and their proton−proton couplings, proven by detailed double decoupling (Figures S24 and S26 in SI) and by COSY experiments (Figures S30−S32 in SI), shows that the C2′ substituent is the C7′ methine carbon. The NOE enhancement (∼12%, corresponds to *ca*. 2.6 Å) between H6 (thymine) and H3′ (Figures S35 and S36 in SI), of **12a/12b**, in addition to $^{3}J_{H1',H2'} = 0$ Hz, further confirms that the sugar is indeed locked by the fused carbocycle in the North conformation as observed for other North-locked nucleosides such as ENA,[13] LNA,[12] and aza-ENA.[20] This further shows that the 1-thyminyl moiety is in β-configuration and anti-conforma-

(65) Barton D, H. R.; Mccombie, S. W. *J. Chem Soc., Perkin Trans. 1* **1975**, 1574.

tion across the glycoside bond. The fact that the NOE enhancement of 6.5% for H1′ upon irradiation on CH_3 at C7′ of **12a** (Figure S35 in SI) is found, shows that the methyl group on C7′ is in close proximity of H1′ (*ca.* 2.8 Å), thereby confirming the *R*-configuration for C7′. The NOE enhancement of 4.5% for H7′ in **12b** (Figure S36 in SI) upon irradiation on H1′, on the other hand, confirms that the H7′ is in close proximity of H1′ (*ca.* 2.2 Å) and hence the *S*-configuration is assigned for C7′. $^2J_{HC}$ HMBC correlations between H7′ and C2′ for compounds **12a**/**12b** (Figures S38 and S39 in SI) unequivocally proves that the oxa-bicyclo[2.2.1]heptane ring system has been formed in the ring-closure reaction (Scheme 1).

For compound **23**, the upfield H2′ shift at δ 2.26 along with H8′ at δ 2.20 and their vicinal proton−proton couplings, proven by the double decoupling (Figure S58 in SI) as well as COSY experiments (Figures S62 and S63 in SI), shows that the C2′ substituent is the C8′ methine carbon. Strong NOE enhancement (8.6%, corresponding to *ca.* 2.6 Å) between H6 (thymine) and H3′ (Figure S66 in SI) in compound **23**, in addition to $^3J_{H1',H2'} = 0$ Hz, further confirms that the sugar is indeed locked in the North-type conformation and that the 1-thyminyl moiety is in β-configuration and anti conformation across the glycoside bond. The NOE enhancement of 3.0% for H1′ upon irradiation at CH_3-(C8′) (Figure S66 in SI) proved that the CH_3(C8′) group is in close proximity of H1′; hence, the C8′ chiral center is in *R*-configuration. Vicinal coupling of H2′ with H8′ as evidenced by double decoupling experiments (Figure S58 in SI) and COSY spectra (Figures S62 and S63 in SI) also unequivocally showed that the bicyclo[3.2.1]octane ring system has indeed been formed in the ring-closure reaction (Scheme 2). This evidence was further corroborated by the observation of the long range ^{1}H−^{13}C connectivity of H8′ with C2′, C3′, and C1′, that of H7′ with C2′, and that of H2′ with CH_3(C8′), C7′, and C8′ in the HMBC experiment. (Figures S68 and S69 in SI).

Detailed NMR characterization by 1D and 2D NMR spectra to show the fused carbocyclic nature of compounds **12a**, **12b**, and **23** are available in SI including chemical shifts in Tables S1 and S2 in SI, spin−spin simulations (Figures S25, S27, and S59 in SI), COSY (Figures S30−32, S62, and S63 in SI) and TOCSY (Figures S33, S34, S64, and S65 in SI) to show the proton−proton connectivity, HMQC (Figure S37, S67 in SI) to show proton−carbon connectivity, and finally HMBC (Figure S38, S39, S68, and S69 in SI) to establish long-range proton−carbon correlation on the basis long-range coupling constant to unequivocally prove the formation of the bicyclic system in **12a**/**12b** as well as in **23**. For the complete NMR characterization of compounds **12a**/**12b** and **23**, see Discussion S1 in SI.

5.0. Molecular Structures of Carbocyclic-LNA-T and Carbocyclic-ENA-T Based on NMR, *ab Initio*, and MD Calculations. Initial dihedral angles from the observed $^3J_{H,H}$ couplings (Table S2 in SI) had been derived (Step I) using the Haasnoot−de Leeuw−Altona generalized Karplus equation[66,67] (Table S3 in SI) and utilized as constraints in the NMR-constrained simulated annealing (SA) molecular dynamics (MD) simulation (0.5 ns, 10 steps) followed by 0.5 ns NMR constrained simulations using torsional constraints to yield NMR-defined molecular structures of the respective compounds (for details of theoretical simulations see Experimental Section). Our combined theoretical and experimental analyses have shown that the sugar pucker conformation in **12a**, **12b**, and **23** is indeed restricted to North-type and both the ENA- and LNA-type carbocyclic analogues have the sugar moiety locked in exactly the same North conformation as in the ENA-T,[13] aza-ENA-T,[20] LNA-T,[12] and 2′-amino-LNA-T[16] counterparts. Further details on the investigation of the nature of the major and minor isomers of carbocyclic-LNA-T (compounds **12a** and **12b**) and conformations of the aglycon and six-membered ring in carbocyclic-ENA-T (**23**) are provided in SI (Discussions S1 and S2 as well as in Table S3 and S4 and Figures S73−S75 in SI).

6.0. Synthesis and Thermal Denaturation Studies of AONs 1−17. The phosphoramidites **14** and **23** were incorporated as mono substitution in a 15 mer DNA sequence through automated synthesis on Applied Biosystems 392 RNA/DNA synthesizer for further studies. The stepwise coupling yields of the modified phosphoramidite were ≈96% and 98%, respectively. Dicyanoimidazole was used as the activating agent for **14**, whereas tetrazole was used to activate **23** with 10 min coupling time for modified phosphoramidites, followed by deprotection of all base-labile protecting groups with 33% aqueous ammonia at 55 °C to give **AONs 1−17** (Table 1). The sequence is targeted to the coding region of the SV40 large T antigen (TAg)[68,69] and has been used in the study of antisense activity of (N)-methanocarba-T-substituted oligonucleotide[70] and as well as in the study of antisense and nuclease stability assays of oxetane[71]-modified, azetidine[18]-modified, and aza-ENA[20]-modified oligonucleotides.

Thermal denaturation studies of AONs (Table 1) containing carbocyclic-LNA-T or carbocyclic-ENA-T have showed an increase of 3.5 to 5 °C/modification (AONs **6**−**9** in Table 1) and 1.5 °C/modification (AONs **10**−**13** in Table 1), respectively, for the AONs duplexes with complementary RNA. However, a net decrease of 1 to 5 °C/modification has been observed for the AONs duplexes with complementary DNA. This may be due to increase in steric clash in the shallow minor groove of AON/DNA duplex. A comparative study of carbocyclic-LNA-T with LNA-T in our lab showed only ∼ 1 °C decrease in T_m with complementary RNA (Table 1) which is indeed surprising meaning that the lack of hydrophilic substituent at 2′ (as in LNA) does not impart any significant decrease in duplex stability with complementary RNA. A comparison of six-membered carbocyclic-ENA-T with aza-ENA-T[20] counterpart has not shown any sequence dependent change in T_m (+1.5 °C/modification independent of the sequence) while in the case of aza-ENA-T[20] containing counterpart the T_m significantly varied (2.5−4.0 °C/modification) depending on the sequence.

7.0. Stability of the Carbocyclic-Modified AONs in Human Blood Serum. The stability of AONs toward various exo- and endonucleases is necessary in order to develop therapeutic oligonucleotides (antisense,[2] RNAi,[72] microRNA[73,74] or triplex-

(66) Haasnoot, C. A. G.; de Leeuw, F. A. A. M.; Altona, C. *Tetrahedron* **1980**, *36*, 2783−2792.
(67) Altona, C.; Sundaralingam, M. *J. Am. Chem. Soc.* **1972**, *94* (23), 8205−1822.
(68) Graessmann, M.; Michaels, G.; Berg, B.; Graessmann, A. *Nucleic Acids Res.* **1991**, *19* (1), 53−9.
(69) Wagner, R. W.; Matteucci, M. D.; Lewis, J. G.; Gutierrez, A. J.; Moulds, C.; Froehler, B. C. *Science* **1993**, *260* (5113), 1510−13.
(70) Marquez, V. E.; Siddiqui, M. A.; Ezzitouni, A.; Russ, P.; Wang, J.; Wagner, R. W.; Matteucci, M. D. *J. Med. Chem.* **1996**, *39* (19), 3739−3747.
(71) Pradeepkumar, P. I.; Chattopadhyaya, J. *J. Chem. Soc., Perkin Trans. 2* **2001**, 2074−2083.
(72) Grunweller, A.; Wyszko, E.; Bieber, B.; Jahnel, R.; Erdmann Volker, A.; Kurreck, J. *Nucleic Acids Res.* **2003**, *31* (12), 3185−3193.
(73) Ambros, V. *Cell (Cambridge, MA, U.S.)* **2001**, *107* (7), 823−826.
(74) Ruvkun, G. *Science (Washington, DC, U.S.)* **2001**, *294* (5543), 797−799.

Table 1. Thermal Denaturation of Native and Modified AONs in the Duplexes with Complementary RNA or DNA Targets[a]

AON	sequence	T_m/°C with RNA§	ΔT_m	T_m/°C with DNA§	ΔT_m*	MALDI-MS found/calcd $[M + H]^+/(m/z)^+$
1	3-d(CTTCTTTTTTACTTC)-5	44		45		4449.7/4448.7
2	3-d(CTT$_{(LNA)}$CTTTTTTACTTC)-5	48	+4	47	+2	4475.48/4474.43
3	3-d(CTTCTT$_{(LNA)}$TTTTACTT C)-5	49	+5	46.5	+1.5	4475.48/4474.43
4	3-d(CTTCTTTT$_{(LNA)}$TTACTTC)-5	49	+5	45.0	0.0	4475.48/4474.43
5	3-d(CTTCTTTTTT$_{(LNA)}$ACTTC)-5	49	+5	46	+1	4475.48/4474.43
6	3-d(CTT$_{(5-carbo)}$CTTTTTTACTTC)-5	47.5	+3.5	45	0.00	4489.40/4488.75
7	3-d(CTTCTT$_{(5-carbo)}$TTTTACTTC)-5	49	+5	44	−1.00	4489.26/4488.75
8	3-d(CTTCTTTT$_{(5-carbo)}$TTACTTC)-5	48	+4	44	−1.00	4489.21/4488.75
9	3-d(CTTCTTTTTT$_{(5-carbo)}$ACTTC)-5	47.5	+3.5	43.0	−2.00	4489.45/4488.75
10	3-d(CTT$_{(6-carbo)}$CTTTTTTACTTC)-5	45.5	+1.5	43.5	−1.5	4503.42/4502.75
11	3-d(CTTCTT$_{(6-carbo)}$TTTTACTTC)-5	45.5	+1.5	39.5	−5.5	4503.25/4502.75
12	3-d(CTTCTTTT$_{(6-carbo)}$TTACTTC)-5	45.5	+1.5	40.0	−5.0	4503.37/4502.75
13	3-d(CTTCTTTTTT$_{(6-carbo)}$ACTTC)-5	45.5	+1.5	39.5	−5.5	4503.26/4502.75
14	3-d(CTT$_{(aza-ENA)}$CTTTTTTACTTC)-5	48	+4	44.5	−0.5	4489.7/4491.1
15	3-d(CTTCTT$_{(aza-ENA)}$TTTTACTTC)-5	46.5	+2.5	42.5	−2.5	4489.7/4490.7
16	3-d(CTTCTTTT$_{(aza-ENA)}$TTACTTC)-5	47.5	+3.5	42	−3	4489.7/4490.7
17	3-d(CTTCTTTTTT$_{(aza-ENA)}$ACTTC)-5	48	+4	42	−3	4489.7/4490.8

[a] T_m values measured as the maximum of the first derivative of the melting curve (A_{260} vs temperature) and are average of at least three runs recorded in medium salt buffer (60 mM Tris-HCl at pH 7.5, 60 mM KCl, 0.8 mM $MgCl_2$, and 2 mM DTT) with temperature range 20 to 70 °C using 1 μM concentrations of the two complementary strands; $\Delta T_m = T_m$ relative to RNA compliment; $\Delta T_m{}^* = T_m$ relative to DNA compliment. T_m performed with complementary DNA or RNA strand. Abbreviations: T$_{(LNA)}$: LNA-T[12](compound **A** in Figure 1); T$_{(5-carbo)}$: carbocyclic-LNA-T (compound **12**, Scheme 1); T$_{(6-carbo)}$: carbocyclic-ENA-T (compound **23**, Scheme 2); T$_{(aza-ENA)}$: aza-ENA-T.[20] (compound **I** in Figure 1).

ing agents[3]). The first generation nuclease resistant antisense phosphorothioates[7] were followed by 2′-O-alkylated modifications.[31] Recent conformationally constrained molecules (LNA,[75−77] ENA,[13] bicyclic,[70] and tricyclic,[78] aza-ENA,[20] oxetane,[71] azetidine,[18] etc.) have also shown enhanced nuclease stability as compared to the natural deoxy counterpart. Egli et al.[79] have demonstrated that charge effects and hydration properties are important factors in influencing the nuclease stability of AONs with a normal phosphodiester backbone. Here, we report a comparative study involving our carbocyclic-LNA (**12a**/**12b**) and carbocyclic-ENA (**23**)-modified AONs (Table 1) with those of LNA and aza-ENA-modified AONs in human blood serum which is mainly composed of 3′-exonucleases.

Modified sequences (Table 1), ^{32}P-labeled at 5′-ends, were digested in human blood serum at 21 °C as shown in the PAGE autoradiograms (Insets A, B, C, and D in Figure 4). In order to understand the extent of transmission of the stereoelectronic effects of the modified locked sugar to the neighboring nucleotides toward the 3′- or at the 5′-end, we introduced modifications further away from the 3′-end of the AONs. The assessment of the modified AON stability in blood serum, owing to various modifications, T$_{(LNA)}$ versus T$_{(aza-ENA)}$ versus T$_{(5-carbo)}$ versus T$_{(6-carbo)}$, *vis-à-vis* the native counterpart (AON **1**), becomes very clear as we compare the digestions with (i) AONs **2** [with T$_{(LNA)}$], (ii) AON **6** [with T$_{(5-carbo)}$], and (iii) AON **10** [with T$_{(5-carbo)}$] and AON **14** [with T$_{(aza-ENA)}$], each having a specific single modification at the position 3 from the 3′-end (Table 1), showing that the site of the 3′-exonuclease-promoted hydrolysis in blood serum was dictated by the site of the incorporation of the modification in the AON (Table 1).

The observations are as follows: (i) the modified AON **2** (full length AON = '*n*') with T$_{(LNA)}$ at position 3 from the 3′-end gave the $n - 1$ fragment in 35 min, and $n - 2$ fragment in 5 h as the major product, which was then completely degraded in 9 h to give various fragments ranging from $n - 2$ to $n - 8$ (Inset **A** in Figure 4). Thus, a comparison of the blood serum cleavage pattern of the native AON **1** with that of the LNA-modified AON **2** showed that the latter is only slightly more stable than the native counterpart. (ii) On the other hand, the modified AON **14** with T$_{(aza-ENA)}$[20] at position 3 from the 3′-end showed full hydrolysis of the 3′-terminal nucleotide within 5 h to give the AON fragments with an $n - 1$ (*ca*. 85%) and $n - 2$ sequence (*ca*. 15%), which were further hydrolyzed to *ca*. 65% and 35% respectively after 12 h. No further cleavage had been observed until 48 h (Inset D in Figure 4 and plots of percent AONs remaining as a function of time in Figure S78 in SI). This means that AON **14** with an $n - 1$ nucleotide sequence was being hydrolyzed steadily to give the AON with an $n - 2$ nucleotide sequence. (iii) In contradistinction, the isosequential AONs with the five- and six-membered carbocyclic modifications [AON **6** with T$_{(5-carbo)}$ and AON **10** with T$_{(6-carbo)}$] showed only one cleavage site to give a single AON product with $n - 1$ nucleotide after 2 h, *which remained completely stable until 48 h* (PAGE autoradiograms in Insets B and C in Figure 4 for up to 48 h, and plots of percentage AONs remaining versus time are shown in Inset A in Figure S76 and Inset A in Figure S77 in SI). Such blood-serum stabilities were also observed for other AONs with five- and six-membered carbocyclic modifications at position 6 (AONs **7**/**11**), position 8 (AONs **8**/**12**), and position 10 (AONs **9**/**13**) (PAGE autoradiograms in Insets B and C in Figure 4, and plots in Insets B−D in Figures S76 and S77 in SI) as well as for aza-ENA-T containing AONs (**15**/**16**/**17**) (PAGE autoradiograms in Inset D, Figure 4, and plots in Insets B−D in Figure S78). The plots (Figures S76 and S77 in SI) obtained as a result of quantification of the PAGE autoradiograms (Figure 4) in carbocyclic-modified AONs **6** (Inset B in Figure 4) and **10** (Inset B in Figure 4**)** clearly showed that the resistance toward nucleases was transmitted toward the

(75) Braasch, D. A.; Jensen, S.; Liu, Y.; Kaur, K.; Arar, K.; White, M. A.; Corey, D. R. *Biochemistry* **2003**, *42* (26), 7967−7975.
(76) Elmen, J.; Thonberg, H.; Ljungberg, K.; Frieden, M.; Westergaard, M.; Xu, Y.; Wahren, B.; Liang, Z.; Orum, H.; Koch, T.; Wahlestedt, C. *Nucleic Acids Res.* **2005**, *33* (1), 439−447.
(77) Kurreck, J.; Wyszko, E.; Gillen, C.; Erdmann, V. A. *Nucleic Acids Res.* **2002**, *30* (9), 1911−1918.
(78) Steffens, R.; Leumann, C. J. *J. Am. Chem. Soc.* **1999**, *121* (14), 3249−3255.
(79) Egli, M.; Minasov, G.; Tereshko, V.; Pallan, P. S.; Teplova, M.; Inamati, G. B.; Lesnik, E. A.; Owens, S. R.; Ross, B. S.; Prakash, T. P.; Manoharan, M. *Biochemistry* **2005**, *44* (25), 9045−9057.

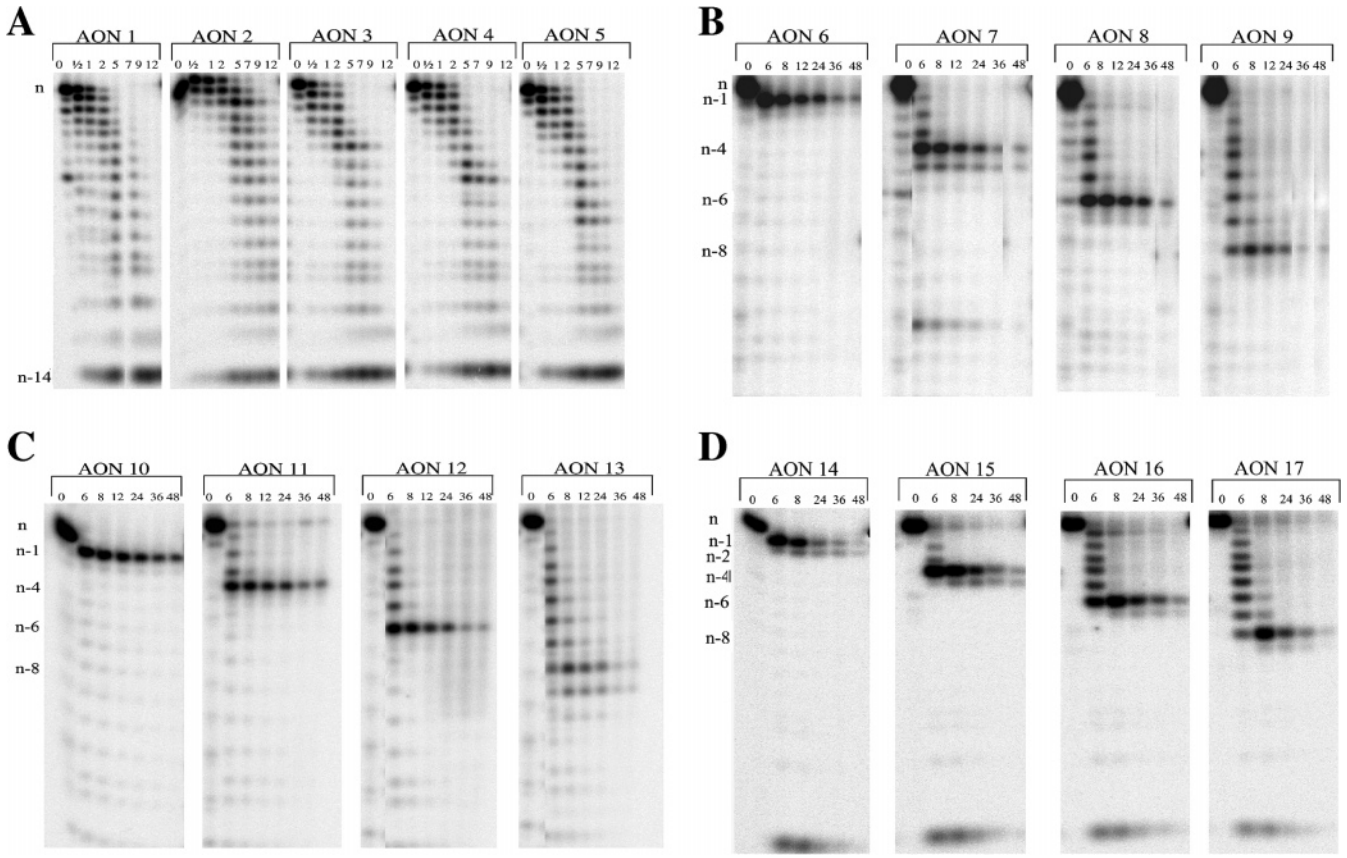

Figure 4. Autoradiograms of 20% denaturing PAGE showing degradation patterns of 5′-^{32}P-labeled AONs in human blood serum (Table 1 for all AON sequences). Inset A: AON **1** and LNA-modified AONs **2**−**5**. Inset B: Carbocyclic-LNA-modified AONs **6**−**9**. Inset C: Carbocyclic−ENA-modified AONs **10**−**13**. Inset D: aza-ENA-modified AONs **14**−**17**. Time points are taken after 0, 1/2, 1 h, 2 h, 5 h, 7 h, 9 h, 12 h, for AONs **1**−**5** and 0 h, 6 h, 8 h, 12 h, 24, 36, and 48 h of incubation for AONs **6**−**17** at 21 °C (see Experimental Section for details).

neighboring 3′ nucleotide of the carbocyclic modification site (i.e., $n - 1$ fragment, when $n =$ full length 15mer AON and the carbocyclic modification site is at position 3 from the 3′-end). In contrast, with the aza-ENA-modified AON **14** (Inset D in Figure 4, Figure S78 in SI) hydrolysis proceeded both at the 3′-phosphate of the modification site and at that of the 3′-neighbor, giving first an $n - 1$ fragment as the predominant product, which was further hydrolyzed with time giving the $n - 2$ fragment (when $n =$ full length 15mer AON and the aza-ENA modification site is at position 3 from the 3′-end). The residual fragments so formed were stable against further hydrolysis for up to 48 h. Similar results were obtained for AONs **7**−**9** (five-membered carbocyclic modifications at position 6, 8, and 10 from the 3′-end giving $n - 4$, $n - 6$, and $n - 8$ fragments, respectively, Figure S76 in SI), AONs **11**−**13** (six-membered carbocyclic modifications at position 6, 8, and 10 from the 3′-end giving $n - 4$, $n - 6$, and $n - 8$ fragments, respectively, Figure S77 in SI) and AONs **15**−**17** (six-membered aza-ENA modifications at position 6, 8, and 10 from 3′-end giving $n - 4/n - 5$, $n - 6/n - 7$, and $n - 8/n - 9$ fragments, respectively. Figure S78 in SI). The fact that in the case of five- and six-membered carbocyclic modifications, the 3′-phosphate of the modified nucleotide was fully stable, whereas the 3′-phosphate of the neighboring residue, which is next to the modified nucleotide at the 3′-end, was unstable and fully hydrolyzed, compared to that of aza-ENA modification in which both 3′-phosphates of the modified nucleotide as well as that of the neighbor residue were unstable, shows that the stereoelectronic effect of the locked sugar into the *N*-type conformation (carbocyclic versus aza-ENA) at the modification site is transmitted differently to alter the phosphate backbone torsions toward the 3′-end thus modulating its susceptibility differently toward hydrolytic cleavage by 3′-nucleases. It is noteworthy that the transmission of the stereoelectronic effect in aza-ENA-T is very comparable to those for oxetane-T-modified and azetidine-T-modified isosequential AONs.

7.1. Mechanism of the Modified AON Stability in Blood Serum. 7.1.1. Effect of 2′-Heteroatom versus 2′-Carbo Substitution in the Modified Nucleotide in the AON. The 3′-terminal nucleotide is hydrolyzed by a 3′-exonuclease in AON substituted by a five- or six-membered carbocyclic residue at position 3 (AONs **6** and **10**) to give only the $n - 1$ fragment. AONs with single substitution at either position 6 (AONs **7** and **11**), 8 (AONs **8** and **12**), or 10 (AONs **9** and **13**) similarly give only $n - 4$, $n - 6$, or $n - 8$ fragments, respectively. The residual AON sequences that remained at the 5′-end of the modification site were found to be intact for more than 48 h in human blood serum (see PAGE autoradiograms in Insets B and **C** in Figure 4, and for plots of percentage of oligonucleotide left as a function of time in Insets A−D in Figures S76 and S77 in SI). However AONs containing a single six-membered aza-ENA-T substitution (i.e., AONs **14**−**17** with single modification incorporated at positions 3, 6, 8, and 10, respectively) showed progressive cleavage with time until the site of modification (Figure 4, Inset D and for plot of percentage of oligonucleotide left as a function time in Insets: A−D in Figure S78 in SI).

This was an interesting observation since the isosequential North-constrained 1′,2′-oxetane[17] or 1′,2′-azetidine[18] with identical modification sites exhibited the 3′-exonuclease-promoted 3′-O−P bond hydrolysis right at the 3′-end of the modification site itself (i.e., at the $n - 2$ site). In contradistinction, isosequential AON with aza-ENA-T modification at position 3 from the 3′-end (i.e., AON **14**) gives predominantly AON with an $n - 1$ residue (Figure 4, Inset D), which is steadily hydrolyzed to give the $n - 2$ product, but the corresponding carbocyclic AONs (AONs **6** and **10**) give only the fully stable $n - 1$ fragment. This suggests that the enzymes of human serum recognize and confer different grades of stability against hydrolysis for relatively more flexible 1′,2′-conformational constraint as in 1′,2′-oxetane[17] or 1′,2′-azetidine[18] compared to the stronger conformational constraints imposed by 2′,4′-modifications as in aza-ENA or in five- and six-membered carbocyclic-ENA/LNA.

Interestingly, a single modification of AON with our carbocyclic-LNA-T or with carbocyclic-ENA-T nucleotides at position 3 from the 3′-end in to the AON **6** or AON **10** has provided the highest degree of exonuclease stability which was earlier achieved by employing four 2′-*O*-[2-(guanidinium)ethyl] (2′-*O*-GE)[29] modifications (including the 3′-terminal modification). Other carbocyclic modifications have also shown nuclease resistance, but less efficiently.[80−83] The 2′- or 6′-alkoxy-substituted carbocyclic nucleotide units (three units at the 3′-end) in the modified AON enhanced stability of AON on fetal calf serum from 2.5 times for [6′α-carbocyclic-2′-deoxy]-T substitution to 24 times for [6′α-carbocyclic-2′-*O*-$(CH_2)_4$-NH_2 or 2′-*O*-$(CH_2)_3$-Ph]-T substitution), compared to that of the native form.[83] It was suggested that replacement of substituents involved in the natural enzyme−substrate complex results in poor recognition and processing by the nucleolytic enzymes, thereby resulting in the nuclease stability. Thus, the nuclease stability was enhanced when a 2′-bulky substituent was introduced in the carbocyclic nucleosides.

The AONs containing five-membered carbocyclic-LNA *versus* AONs with the six-membered carbocyclic-ENA show enhanced, but identical, blood serum stability, thereby showing that the steric bulk is relatively unimportant.[31] This is in sharp contrast to the conclusion drawn by comparison of the LNA versus ENA[24] modified AONs, in that the latter is 2.5−3 times more stable than the former,[13] apparently, according to the authors, owing to an extra methylene linker. The 3′-exonuclease (SVPDE) stability had also been observed to be higher for the 2′-*O*-GE[29] and 2′-*O*-aminopropyl modifications,[84] as well as for the 4′-α-*C*-aminoalkylthymidine AONs,[30] which showed complete nuclease resistance upon incorporation of five modified nucleotides as mixmers, compared to the native counterpart. Notably, nuclease digestion studies involving 4′-α-*C*-aminoalkylthymidine AONs showed that longer chain alkyls were less potent in providing stability against nuclease, and hinted at the role of ammonium ions in providing the stability.[30] Subsequently, it was shown that the native ribonucleoside with a 2′-*O*-alkyl substitutent either by its bulk (pentoxy > propoxy > methoxy > deoxy)[31] or by its stereoelectronic modulation (2′-*O*-GE)[29] of the hydration can bring about nucleolytic stability.

Since our carbocyclic AONs were completely devoid of polar effect at C2′,[28] the above explanations invoking charge or steric effects is not applicable to explain the unprecedented nuclease stability of these carbocyclic AONs in the blood serum. The enhanced stabilities of the carbocyclic-AONs with respect to their bicyclic 2′-*O*-(LNA and ENA) and aza-ENA analogues suggests that the accessibility of water to the 2′-*O*- in LNA or to the 2′-*N*- in the aza-ENA substituent in a modified nucleotide is most probably more important in order to cleave the vicinal 3′-phosphodiester bond by the exonucleases of blood serum.

7.1.2. Solvation Free-Energy Calculation To Elucidate Relative Hydrophobicity of the 2′-Substituent. In order to understand how the nature of 2′-substitution in the modified AON affects the relative access of water to the scissile phosphate, we have analyzed the solvation free-energies of different modified nucleosides (Table S5 in SI) utilizing Baron and Cossi's implementation of the polarizable conductor CPCM model[85] of solvation on the *ab initio* optimized (HF, 6-31G** basis set) molecular geometries. This allowed us to understand the lipophilic *versus* hydrophilic nature of different 2′,4′-constrained modifications in LNA/ENA/2′-amino-LNA/aza-ENA/carbocyclic-LNA/carbocyclic-ENA in a comparative manner. Table S5 in SI thus shows that the energy of solvation of the five-membered (**12a** and **12b**) and six-membered (**23**) carbocyclic nucleosides compared to their oxygen and nitrogen containing counterparts decreases in the following order: six-membered carbocyclic-ENA-T (-12.2 kcal mol^{-1}) > five-membered carbocyclic-LNA-T (-12.9 kcal mol^{-1}) > aza-ENA-T (-15.2 kcal mol^{-1}) > ENA-T (-15.6 kcal mol^{-1}) > LNA-T (-16.8 kcal mol^{-1}). This suggests that our five-membered and six-membered carbocyclic nucleosides, on account of their hydrophobic nature, are not as well solvated as compared to their LNA, ENA, and aza-ENA counterparts, thereby showing that hydration around a scissile phosphate is most probably important for the nuclease-promoted hydrolysis. This leads us to speculate that this hydration around the C2′ substituent with heteroatoms such as 2′-*O*- in LNA or to the 2′-*N*- in aza-ENA in a modified AON is utilized by the exonuclease to capture a water molecule to hydrolyze the 3′O−PO_3^-R bond of the vicinal phosphate, which is not possible with our carbocyclic-AONs.

8.0. 3′-Exonuclease Stability Assay (with snake venom phosphodiesterase). The stability of AONs of carbocyclic analogues of LNA and ENA (Table 1) toward 3′-exonuclease was investigated using snake venom phosphodiesterase over a period of 72 h at 21 °C (PAGE autoradiogram in Figure S79 in SI) and compared with isosequential LNA and aza-ENA modified AONs under identical conditions. The results obtained were similar to that obtained in human blood serum assay (PAGE autoradiogram in Figure 4) showing identical cleavage sites and identical resistance pattern, i.e., cleavage of the phosphodiester bond next to the modification site toward the

(80) Renneberg, D.; Bouliong, E.; Reber, U.; Schumperli, D.; Leumann Christian, J. *Nucleic Acids Res.* **2002**, *30* (13), 2751−2757.
(81) Bolli, M.; Trafelet, H. U.; Leumann, C. *Nucleic Acids Res.* **1996**, *24* (23), 4660−4667.
(82) Perbost, M.; Lucas, M.; Chavis, C.; Pompon, A.; Baumgartner, H.; Rayner, B.; Griengl, H.; Imbach, J. L. *Biochem. Biophys. Res. Commun.* **1989**, *165* (2), 742−747.
(83) Altmann, K.-H.; Bevierre, M.-O.; De Mesmaeker, A.; Moser, H. E. *Bioorg. Med. Chem. Lett.* **1995**, *5* (5), 431−436.
(84) Teplova, M.; Wallace, S. T.; Tereshko, V.; Minasov, G.; Symons, A. M.; Cook, P. D.; Manoharan, M.; Egli, M. *Proc. Natl. Acad. Sci. U.S.A.* **1999**, *96* (25), 14240−14245.
(85) Barone, V.; Cossi, M. *J. Phys. Chem. A* **1998**, *102* (11), 1995−2001.

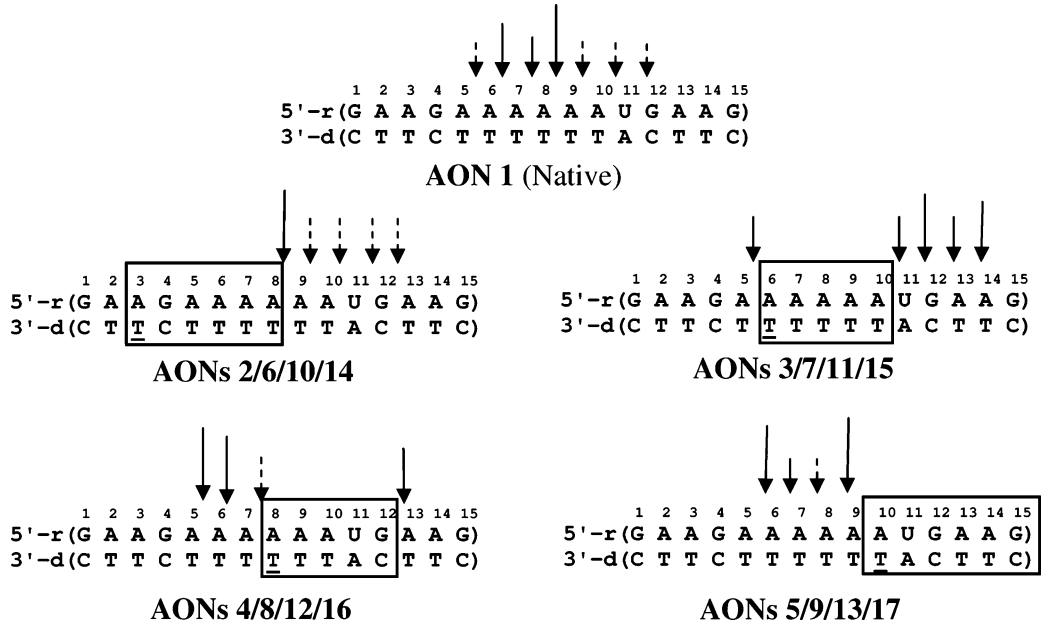

Figure 5. The RNase H1 cleavage pattern of AONs **1**−**17**/RNA heteroduplexes. Vertical arrows show the RNase H cleavage sites, with the relative length of the arrow showing the extent of the cleavage. The square boxes around a specific sequence shows the stretch of the RNA, which is resistant to RNase H cleavage thereby giving footprints (see PAGE autoradiograms in Figure 6).

3′ end and subsequent resistance to degradation for up to 72 h (PAGE autoradiogram in Figures S79 in SI and plots of percentage of oligonucleotide left as function of time in Figures S80−S82 in SI). These experiments clearly show that the effect of a hydrophobic environment imparted by the carbocyclic analogues of LNA and ENA is important in dictating the nuclease stability of the modified AON.

9.0. RNase H Digestion Studies. In the antisense strategy, the RNase H recruitment by the modified AON, with long nuclease stability as exhibited by our carbocyclic modifications, and the target RNA heteroduplexes is an important step for the design of potential therapeutics for engineering a specific gene silencing effect.[2]

Hence, RNase H-mediated cleavage of the RNA strand complementary to the modified AON strands **2**−**17** (with carbocyclic-LNA, carbocyclic-ENA, aza-ENA, and LNA modifications) has been studied here, using the native AON/RNA duplex as a reference, in order to address the issue if the recruitment of RNase H by the heteroduplexes is in anyway compromised as a result of carbocyclic modifications incorporated in the AON strand. We have used *E. coli* RNase H in our studies on account of its availability, and the fact that its properties are known to be not very different from the mammalian enzyme.[77] The, RNA complementary to AONs (AONs **1**−**17** in Table 1) formed duplexes and were found to be good substrates for RNase H but with varying cleavage sites (Figure 5) depending on the site of modification in the AON strand as shown in PAGE autoradiograms (Insets A−D in Figure 6). The main observations are as follows:

(i) The RNA complement of the unmodified native AON **1**/RNA duplex was cleaved quite randomly with a slight preference after A-8 position.

(ii) For the isosequential AONs with single modification at different sites (Table 1) containing either LNA (AONs **2**−**5**), carbocyclic-LNA-T (AONs **6**−**9**), carbocyclic-ENA-T (AONs **10**−**13**), or aza-ENA-T AONs **14**−**17**) modifications showed uniquely identical cleavage footprint patterns having 5−6 nt gaps (Insets A−D in Figure 6). It is remarkably surprising that the RNase H enzyme could not distinguish the functional differences exhibited by the North-conformationally constrained LNA, carbocyclic-LNA, carbocyclic-ENA, and aza-ENA modifications, compared to nucleases.

This suggests that the RNase H does not recognize the hydrophobic (as in carbocyclic-LNA, carbocyclic-ENA) or hydrophilic (LNA and aza-ENA) character of the substituent at the 2′-position of the modified nucleosides, but interrogates only at the subtle difference in the flexibility of the North-type sugar puckering (2′,4′ versus 1′,2′) in that we observed different cleavage sites and footprint pattern (4−5 nt gaps) for isosequential 1′,2′-constrained North-East sugar puckered oxetane[71] and azetidine[18] modified AONs compared to those of the more rigid 2′,4′-constrained systems (LNA, carbocyclic-LNA, carbocyclic-ENA, and aza-ENA modified AONs).

The cleavage rates of RNase H digestion were determined by densitometric quantification of gels and subsequently by plotting the uncleaved RNA fraction as a function of time (Insets E−H in Figure 6). The reaction rates were obtained by fitting the degradation curves to single-exponential decay functions.[77] The relative cleavage rates with carbocyclic-LNA, carbocyclic-ENA, aza-ENA, and LNA modified AON/RNA duplexes were found to be very similar to that of the native counterpart irrespective of the type and the site of modification in the AON strand (compare the relative rates in Figure 7).

The main conclusion which can be drawn from these studies is that even though all AONs used (Table 1) recruited RNase H almost as efficiently as that of the native counterpart (Figure 7), it is only the carbocyclic-LNA and the carbocyclic-ENA modified AONs (AON **6**−**13**) which have shown (Figure 4) much enhanced nuclease stability in the blood serum (ca. 48 h) as compared to that of the native and the LNA-modified AONs (fully degraded <12 h) and aza-ENA (≈85% stable in 48 h) (Figure 8, Figures S76−S78 in SI). Clearly, the enhanced

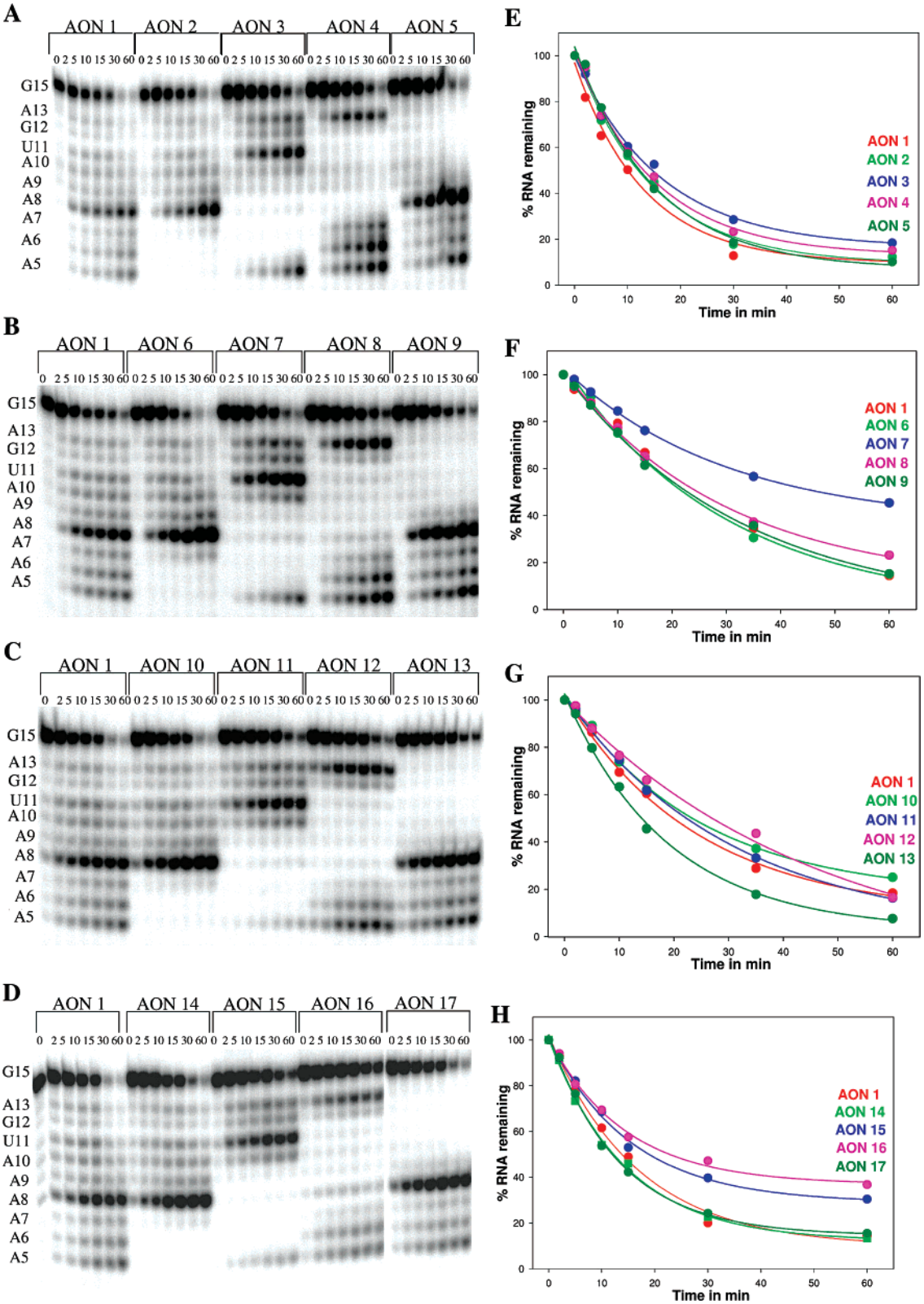

Figure 6. Autoradiograms of 20% denaturing PAGE, showing the cleavage kinetics of 5′-^{32}P-labeled target RNA by *E. coli* RNase H1 in the AONs **1**−**17** after 2, 5, 10, 15, 30, and 60 min of incubation. Conditions of cleavage reactions: RNA (0.8 μM) and AONs (4 μM) in buffer containing 20 nM Tris-HCl (pH 8.0), 20 mM KCl, 10 mM $MgCl_2$, and 0.1 mM DTT at 21 °C; 0.04 U of RNase H1. Inset A: LNA-T modified AONs **2**−**5** with native AON **1**. Inset B: carbocyclic-LNA-T modified AONs **6**−**9**. Inset C: carbocyclic-ENA-T modified AONs **10**−**13** with native AON **1**. Inset D: aza-ENA-T modified AONs **14**−**17** with native AON **1**. The graphs in Insets E, F, G, and H show the kinetics of RNase H1-mediated cleavage of the target RNA, the remaining fraction of target RNA is measured densitometrically and plotted as a function of time fitted to a single-exponential decay function. Inset E: AON **1** with AONs **2**−**5**. Inset F: for AON **1** with AONs **6**−**9**. Inset G: AON **1** and AONs **10**−13. Inset H: AON **1** and AONs **14**−**17**.

lifetime of these carbocyclic-modified AONs in the blood serum (Figure 8, Figures S76−S78 in SI) may produce the highly desired pharmacokinetic properties because of their stability and consequently a net reduction of the required dosage. This makes

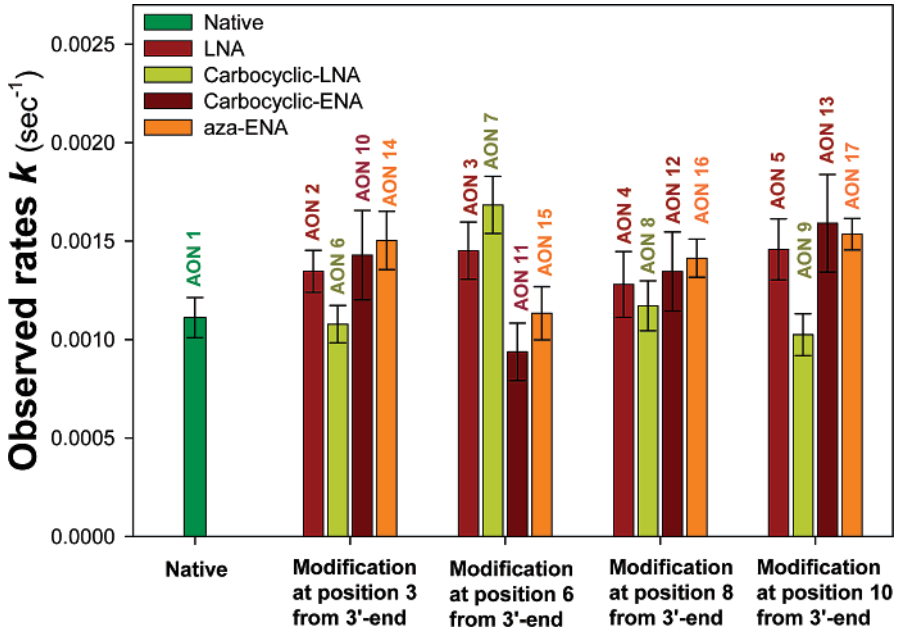

Figure 7. Bar plots of the observed cleavage rates of the RNase H promoted degradation of AONs **2**−**17**/RNA heteroduplexes with various modifications (LNA-T, carbocyclic-LNA-T, carbocyclic-ENA-T, and aza-ENA-T) in the AON strand at position 3, 6, 8, and 10 from the 3′-end, in comparison to that of the native counterpart AON **1**. The observed initial cleavage rates (s^{-1}) of AONs **1**−**17**/RNA heteroduplexes by *E. coli* RNase H are found to be very similar, while in the human blood serum (Figures 8−11) the degree of stability varied widely for the carbocyclic *versus* heterocyclic modified AONs reflecting their respective hydrophobic/hydrophilic properties.

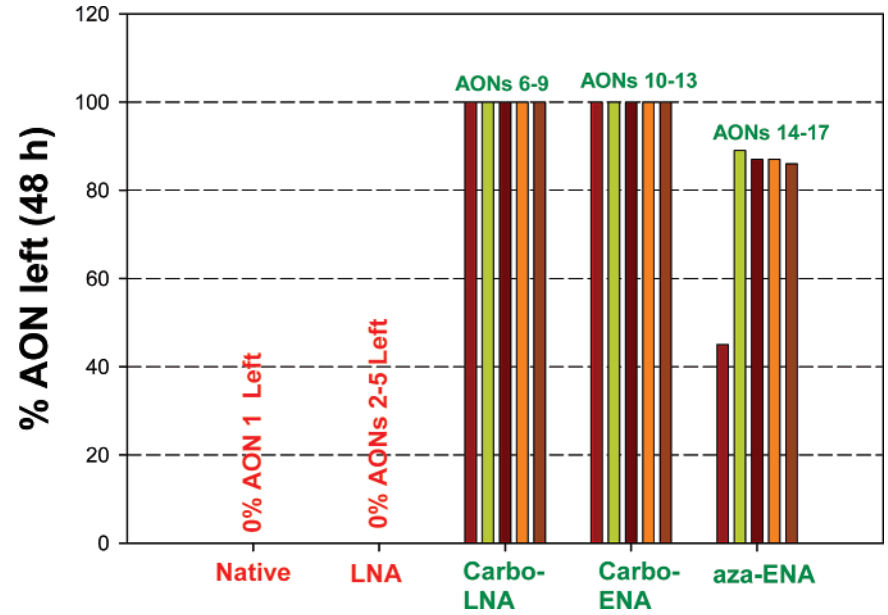

Figure 8. The percent of AONs **6**−**17** left after 48 h of incubation in the human blood serum at 21 °C. Note that, under similar condition, the native (AON **1**) and LNA-containing AONs (AONs **2**−**5**) were fully degraded after 12 h, and shown in blank (red colored). Note that the human blood serum stable product (i) is (n − 1) for the AONs **6/10/14** (AONs substituted at position 3 from the 3′-end) after the hydrolysis of the 3′-terminal nucleotide, (ii) (n − 4) product for the AON **7/11/15** (AONs substituted at position 6 from the 3′-end), (iii) the (n − 6) product for the AONs **8/12/16** (AONs substituted at position 8 from the 3′-end), whereas (iv) the (n − 8) product was formed from AONs **9/13/17** (AONs substituted at position 10 from the 3′-end). Thus the concentration of these final hydrolysis products formed as a result of introduction of a specific modification at a particular site was taken as 100%. Also note: cleavage of one nucleotide from the 3′-end is (n − 1), and the cleavage of two nucleotides from the 3′-end is (n − 2), and so on, where 'n' is the full length AON.

our carbocyclic-LNA, carbocyclic-ENA, and aza-ENA modified AONs the best candidates for antisense therapeutics because of their efficient exploitation in the enzymatic turnover. In this context, it may be noted that the modified AONs with all thymidines replaced with the conformationally constrained (North- or South-locked) 2′-deoxy-methanocarba-nucleoside[70] or LNAs[77] or tricyclo-DNA[80] did not recruit RNase H.

Conclusions

1. In order to develop gene silencing agents with natural phosphodiester linkages, three factors are perhaps most important: stability, delivery, and RNase H recruitment. In this regard, we have designed and synthesized AONs containing five-membered (**12a**/**12b**) and six-membered (**23**) carbocyclic analogues of LNA (carbocyclic-LNA-T) and ENA (carbocyclic-

ENA-T), which are both nuclease resistant and capable of eliciting an RNase H response.

2. The synthesis of these novel conformationally constrained carbocyclic analogues have been achieved using free-radical C−C bond formation as a key step. Various NMR experiments including ^{1}H homodecoupling experiments, 1D nuclear Overhauser effect spectroscopy (1D NOESY), 2D total correlation spectroscopy (TOCSY), 2D COSY, and ^{13}C NMR experiments, including distortionless enhancement by polarization transfer (DEPT), as well as long-range ^{1}H−^{13}C HMBC correlation ($^2J_{H,C}$ and $^3J_{H,C}$), and one-bond heteronuclear multiple-quantum coherence (HMQC) have been employed to show unambiguously that indeed a carbon−carbon bond formation has taken place between C2′ and the olefinic side chain tethered at C4′ to give the North-type conformationally constrained bicyclic nucleosides.

3. The molecular structures of the five-membered (**12a**/**12b**) and six-membered (**23**) carbocyclic analogues have also been studied using *ab initio* and MD simulations to understand the structural reasons behind the regio- and stereochemistry of the cyclization products.

4. Sixteen single modified AONs (15mer) containing the carbocyclic analogues (carbocyclic-LNA-T and carbocyclic-ENA-T) and aza-ENA[20] modification have been tested and have shown good target affinity as shown by the increase (compared to the native counterpart) in thermal stability of duplexes with their complementary RNAs (T_m increase by 3.5−5 °C and 1.5 °C/modification) for carbocyclic-LNA-T and carbocyclic-ENA-T, respectively.

5. The AONs containing the carbocyclic analogues of ENA and LNA have shown unprecedented nuclease stability, starting from the 3′-neighboring nucleotide of the modification site till the 5′-end; thus, the nuclease stable part of the AON depends upon where the site of the modification is introduced in the modified AON.

6. The modified AONs have shown recruitment of RNase H almost as efficiently as by native deoxy/RNA duplexes and brought about degradation of the RNA target.

7. A comparison of the nuclease stability of carbocyclic analogues with LNA and aza-ENA and its correlation with the energy of solvation indicates that it is the relative hydrophobicity of the carbocyclic modification leading to a change of hydration pattern around the modified nucleotide in the AONs which is probably responsible for the high nuclease stability of the modified AONs.

Implication. Remarkably, a single incorporation of carbocyclic-LNA/-ENA-T into AONs leads to very much more enhanced nuclease stability in the blood serum (stable >48 h) [compared to those of the native (fully degraded <3 h) and the LNA-modified AONs (fully degraded <9 h) and aza-ENA (≈85% stable in 48 h)]. This enhanced stability of the carbocyclic-LNA/-ENA-T-containing AONs however do not compromise the recruitment of the RNase H to cleave the complementary RNA in the modified AON/RNA heteroduplex, compared to that of the native. This enhanced lifetime of these carbocyclic-modified AONs in the blood serum may produce the highly desired pharmacokinetic properties and consequently a reduction of the required dosage and the toxicity while down-regulating a message *in vivo*, which may make the carbocyclic-LNA and carbocyclic-ENA modifications excellent candidates as potential antisense or RNAi therapeutic agents.

Experimental Section

3,5-Di-*O*-benzyl-4-*C*-vinyl-1,2-*O*-isopropylidene-α-D-ribofuranose (4). Oxalyl chloride (10.7 mL, 125 mmol) was added to dichloromethane (350 mL) cooled at −78 °C. DMSO (15 mL, 200 mmol was added dropwise to this solution over 30 min. After stirring for 20 more min a solution of **2** (20 g, 50 mmol) in dichloromethane (100 mL) was added dropwise to this mixture in about 20 min and stirred at −78 °C for another 30 min. DIPEA (60 mL, 350 mmol) was added to this cooled mixture and allowed to warm to room temperature. Water was added to the reaction and twice extracted with dichloromethane (100 mL). The organic layer was washed with water and brine, dried over $MgSO_4$, and concentrated under reduced pressure. In another reaction BuLi (1.6 M solution in hexane, 95 mL, 150 mmol) was added to a precooled suspension of methyl-triphenylphosphonium bromide (54 g 150 mmol) at 0 °C in dry THF and stirred at room temperature for 1 h. The yellow solution so obtained was cooled to −78 °C and a solution of crude aldehyde in dry THF was then added dropwise in about 20 min and stirred at −78 °C overnight. The reaction was quenched with saturated aqueous NH_4Cl, stirred for about 1 h at room temperature, extracted with ether (3 × 200 mL), dried over $MgSO_4$ and, concentrated under reduced pressure. The crude material was purified by column chromatography on silica gel (0−10% ethyl acetate in cyclohexane, v/v) to give **2** as a colorless oil (17 g, 43 mmol, 87%). R_f = 0.60 (20% ethyl acetate in cyclohexane, v/v). ^{1}H NMR (600 MHz, $CDCl_3$) δ: 7.3 (10 H, m), 6.20 (1H, dd, $J_{H6,H7}$ = 11 Hz, 18 Hz, H6), 5.76 (1H, d, $J_{H1,H2}$ = 3.9 Hz, H1), 5.22 (1H, dd, 1.8 Hz, 17.5 Hz, H7), 5.25 (1H, dd, J = 1.8 Hz, 11 Hz, H7), 4.76 (1H, d, J_{gem}= 12 Hz, CH_2Bn), 4.59 (1H, d, J_{gem}= 12 Hz, CH_2Bn), 4.57 (1H, app t, J = 4.6 Hz, H2), 4.5 (1H, d, J_{gem}= 12 Hz, CH_2Bn), 4.40 (1H, d, J_{gem} = 12 Hz, CH_2Bn), 4.25 (1H, d, J = 4.9 Hz, H3), 3.32 (2H, s, H5), 1.52 (3H, s, CH_3), 1.28 (3H, s, CH_3); ^{13}C NMR (125.7 MHz) δ: 138.0, 137.8, (Bn), 135.4 (C6), 128.3, 127.9, 127.8, 127.5 (aromatic), 116.3(C7), 113.3, 103.8 (C1), 86.4 (C4), 78.3 (C2), 77.2 (C3), 73.4 (CH_2Bn), 72.7 (C5), 72.4 (CH_2Bn), 26.0 (CH_3), 25.6 (CH_3).

3,5-Di-*O*-benzyl-4-*C*-hydroxyethyl-1,2-*O*-isopropylidene-α-D-ribofuranose (5). To a solution of **2** in dry THF (200 mL) was added 0.5 M solution of 9-BBN (250 mL, 128 mmol), and the mixture was stirred overnight. Water was added till gas evolution stopped, 3 N NaOH solution (50 mL) was added, and then slowly 33% aqueous H_2O_2 was added while the temperature was maintained at about 50 °C. The mixture was stirred for about 30 min at room temperature and then partitioned between ethyl acetate and water and extracted twice with ethyl acetate (100 mL). The organic layer was dried, evaporated, and purified over silica gel (20−30% ethyl acetate in cyclohexane, v/v) to give **5** as colorless oil (16 g, 39 mmol, 95%). R_f = 0.40 (5% methanol in dichloromethane, v/v). ^{1}H NMR (270 MHz, $CDCl_3$) δ: 7.3 (10H, m), 5.75 (1H, d, $J_{H1,H2}$ = 4 Hz, H1), 4.77 (1H, d, J_{gem} = 12 Hz, CH_2-Bn), 4.67 (1H, app t, J = 4.8 Hz, H2), 4.55 (1H, d, J_{gem} = 12 Hz, CH_2Bn), 4.52 (1H, d, J_{gem} = 12 Hz, CH_2Bn), 4.41 (1H, d, J_{gem} = 12 Hz, CH_2Bn), 4.12 (1H, d, $J_{H2,H3}$ = 5.57 Hz, H3), 3.8 (2H, m, H7), 3.51 (1H, d, J = 10.3 Hz, H5), 3.3 (1H, d, J = 10.4 Hz, H5), 3.0 (1H, br s, 7-OH), 2.51 (1H, ddd, J = 3.4 Hz, 6.4 Hz, 15 Hz, H6), 1.80 (1H, ddd, J = 4 Hz, 8.5 Hz, 15 Hz, H6), 1.63 (3H, s, CH_3), 1.31 (3H, s, CH_3); ^{13}C NMR (67.9 MHz, $CDCl_3$) δ: 137.9 (Bn), 127.7, 127.8, 127.9, 128.5 (aromatic), 113.6 (isopropyl), 104.4 (C1), 87.3 (C4), 79.3 (C2), 78.6 (C3), 73.6 (CH_2Bn), 73.3 (C5), 72.5 (CH_2Bn), 58.8 (C7), 34.0 (C6), 26.5 (CH_3), 26.4 (CH_3); MALDI TOF m/z $[M + Na]^+$ found 437.14, calcd 437.19.

4-*C*-Allyl-3,5-di-*O*-benzyl-1,2-*O*-isopropylidene-α-D-ribofuranose (6). Oxalyl chloride (6.2 mL, 72.46 mmol) was added to dichloromethane (200 mL) cooled at −78 °C. DMSO (11 mL, 145 mmol) was added dropwise to this solution over 30 min After stirring for an additional 20 min, a solution of **5** (15 g, 36.23 mmol) in

dichloromethane (100 mL) was added dropwise to this mixture in about 20 min and stirred at −78 °C for another 45 min. DIPEA (35 mL, 200 mmol) was added to this cooled mixture and allowed to warm to room temperature. Water was next added to the reaction and twice extracted with dichloromethane (100 mL). The organic layer was washed with water and brine, dried over $MgSO_4$, and concentrated under reduced pressure. In another reaction BuLi (1.6 M solution in hexane, 78 mL, 126 mmol) was added to a precooled suspension of methyl-triphenylphosphonium bromide (45 g,126 mmol) at 0 °C in dry THF and stirred at room temperature for 1 h. The yellow solution so obtained was cooled to −78 °C, and a solution of crude aldehyde in dry THF was then added dropwise in about 20 min and stirred at −78 °C overnight. The reaction was quenched with saturated aqueous NH_4Cl, stirred for about 1 h at room temperature, extracted with ether (3 × 200 mL), dried over $MgSO_4$, and concentrated under reduced pressure. The crude material was purified by column chromatography on silica gel (0−10% ethyl acetate in cyclohexane, v/v) to give **6** as a yellowish oil (12 g, 29 mmol, 70%). $R_f = 0.60$ (20% ethyl acetate in cyclohexane, v/v). ^{1}H NMR (270 MHz, $CDCl_3$) δ: 7.35 (10H, m, Bn), 5.95 (1H, m, H7), 5.77 (1H, d, $J_{H1,H2} = 4$ Hz, H1), 5.09 (2H, m, H8), 4.78 (1H, $J_{gem} = 12.1$ Hz, CH_2Bn), 4.63 (1H, app t, $J = 4.3$ Hz, H2), 4.58 (1H, d, $J_{gem} = 12.1$ Hz, CH_2Bn), 4.54 (1H, d, $J_{gem} = 12$ Hz, CH_2Bn), 4.41 (1H, d, $J_{gem} = 12$ Hz, CH_2Bn), 4.18 (1H, d, $J_{H2,H3} = 5.2$ Hz, H3), 3.45 (1H, d, $J_{H5,H5} = 10.4$ Hz, H5), 3.32 (1 H, d, $J_{H5,H5} = 10.4$ Hz, H5), 2.96 (1H, dd, $J_{H6,H6} = 14.7$ Hz, $J_{H6,H7} = 7.4$ Hz, H6), 2.39 (1H, dd, $J_{H6,H6} = 14.7$ Hz, $J_{H6,H7} = 8.5$ Hz, H6), 1.60 (3H, s, CH_3), 1.33 (3 H, s, CH_3); ^{13}C NMR (67.9 MHz) δ: 138.3 (Bn), 134.0 (C7), 127.6, 127.8, 128.4, 128.6 (aromatic), 117.6 (C8), 113.3 (isopropyl), 104.2 (C1), 86.4 (C4), 79.6 (C2), 78.3 (C3), 73.5 (CH_2Bn), 72.5 (C5), 72.3 (CH_2Bn), 37.0 (C6), 26.8 (CH_3), 26.3 (CH_3); MALDI-TOF m/z $[M]^+$ Found 410.2, calcd 410.1.

1-[4-*C*-Allyl-3,5-di-*O*-benzyl-2-*O*-acetyl-*β*-D-ribofuranosyl]-thymine (8). Acetic anhydride (17 mL, 175 mmol) and acetic acid (87 mL) were added to **4** (6.0 g, 14 mmol) and cooled, and triflic acid (0.1 mL, 0.7 mmol) was added to it and stirred. After 30 min the reaction was quenched with cold saturated $NaHCO_3$ solution and extracted with dichloromethane. The organic layer was dried and evaporated. The crude was coevaporated with dry CH_3CN thrice and dissolved in the same. Thymine (2.4 g, 19 mmol) and *N*,*O*-bis(trimethylsilyl)acetamide (9.6 mL, 38 mmol) were added to this solution and refluxed for 45 min till the suspension becomes a clear solution. This solution was cooled to 0 °C, and TMSOTf (3.5 mL, 17.5 mmol) was added dropwise and stirred overnight. The reaction was quenched with saturated NH_4Cl solution and extracted with dichloromethane The organic layer dried, evaporated, and chromatographed over silica gel (2−6% methanol in dichloromethane, v/v) to give **8** as a white foam (6 g, 11 mmol, 80%). $R_f = 0.60$ (5% methanol in dichloromethane, v/v). ^{1}H NMR (500 MHz) δ: 7.48 (1H, s, H6), 7.3 (10H, m), 6.25 (1H, d, $J_{H1',H2'} = 5.5$ Hz, H1′), 5.83 (1H, *m*, H7′), 5.41 (1H, app t, 5.5 Hz, H2′), 5.09 (2H, m, H8′, 8″), 4.63 (1H, d, $J_{gem} = 11.5$ Hz, CH_2Bn), 4.50 (1H, d, $J_{gem} = 11.5$ Hz, CH_2Bn), 4.47 (1H, d, $J_{gem} = 11.5$ Hz, CH_2Bn), 4.45 (1H, d, $J_{gem} = 11.5$ Hz, CH_2Bn), 4.37 (1H, d, $J_{2H',3H'} = 5.94$ Hz, H3′), 3.67 (1H, d, $J_{H5',H5''} = 10.5$ Hz, H5″), 3.38 (1H, d, $J_{H5',H5''} = 10.5$ Hz, H5′), 2.65 (1H, dd, $J_{H6,H7} = 6$ Hz, $J_{H6',H6''} = 15$ Hz, H6″), 2.29 (1H, dd, 8 Hz, 14 Hz, H6′), 2.08 (3H, acetyl), 1.49 (3H, CH_3-thymine); ^{13}C NMR (125.7 MHz) δ: 170.1(>C═O acetyl), 163.9 (C4), 150.5 (C2), 135.6, 137 2, 137.5 (aromatic), 132.5 (C6), 127.6, 127.8, 128.0, 128.0, 128.4, 128.6 (aromatic), 118.6 (C8′), 111.3 (C5), 86.9 (C4′), 85.9 (C1′), 77.6 (C3′), 75.1 (C2′), 74.3 (CH_2Bn), 73.5 (CH_2Bn), 72.9 (C5′), 37.2 (C6′), 20.7 (CH_3, acetyl), 11.9 (CH_3, thymine): MALDI-TOF m/z $[M + H]^+$ found 521.14 calcd 521.22.

1-[4-*C*-Allyl-3,5-di-*O*-benzyl-2-*O*-phenoxythiocarbonyl-*β*-D-ribofuranosyl]-thymine (10). Compound **8** (5.0 g, 9.6 mmol) was treated with 27% methanolic ammonia solution overnight. After evaporation of the solvent, the crude was coevaporated thrice with dry pyridine and dissolved in the same. To this precooled solution was added DMAP (1.17 g, 9.6 mmol). Then dropwise was added phenyl chlorothionoformate (1.6 mL, 11.53 mmol), and reaction was stirred overnight. Reaction was quenched with saturated solution of $NaHCO_3$ and extracted with dichloromethane. The organic layer was dried over $MgSO_4$, concentrated, and chromatographed over silica gel (10−30% ethyl acetate in cyclohexane, v/v) to give **10** as yellowish foam (4.1 g, 6.72 mmol, 70%). $R_f = 0.60$ (30% ethyl acetate in cyclohexane, v/v). ^{1}H NMR (600 MHz) δ: 8.58 (1H, s, N−H), 7.48 (1H, s, H6), 7.19 (15H, m), 6.44 (1H, d, $J_{H1',H2'} = 6.1$ Hz, H1′), 5.97 (1H, app t, $J = 5.8$ Hz, H2′), 5.83 (1H, m, H7′), 5.09 (2H, m, H8′-H8′′), 4.77 (1H, d, $J_{gem} = 11.2$ Hz, CH_2Bn), 4.55 (3H, m, CH_2Bn, H3′), 3.71 (1H, d, $J_{H5',H5''} = 10.3$ Hz, H5″), 3.48 (1H, d, $J_{H5',H5''} = 10.3$ Hz, H5′), 2.66 (1H, dd, $J_{H6,H6} = 14.6$ Hz, $J_{H6,H7} = 8.1$ Hz, H6″), 2.35 (1 H, dd, $J_{H6,H6} = 14.6$ Hz, $J_{H6,H7} = 8.1$ Hz, H6′), 1.51 (3H, CH_3, thymine); ^{13}C NMR (125.7 MHz) δ: 194.4 (>C═S), 163.4 (C4), 150.3 (C2), 137.1, 137.2 (aromatic), 135.6 (C6), 132.4 (C7′), 121.6, 126.7, 127.3, 127.6, 127.8, 128.0, 128.1, 128.4, 128.6, 129.3, 129.5(aromatic), 118.8 (C8′), 111.5 (C5′), 87.1 (C4′), 85.1 (C2′), 82.9 (C1′), 77.8 (C3′), 74.9 (C−CH_2Bn), 73.7 (C5′), 73.7 (C−CH_2Bn), 37.3 (C6′), 11.9 (CH_3, thymine); MALDI-TOF m/z $[M + H]^+$ found 615.16 calcd 615.21.

(1*R*,3*R*,4*R*,5*R*,7*S*)-7-Benzyloxy-1-benzyloxymethyl-3-(thymin-1-yl)-2-oxa-bicyclo[2.2.1]heptane (11a/11b). Compound **10** (3.0 g, 4.8 mmol) was dissolved in 150 mL of dry toluene and purged with dry nitrogen for 30 min. Bu_3SnH (1.3 mL, 4.8 mmol) was dissolved in 20 mL of toluene, and half of this solution was added dropwise to refluxing solution in over 30 min. AIBN (0.920 g, 4.8 mmol) was dissolved in 20 mL of dry toluene and added to the above solution dropwise, and simultaneously was added the remaining solution of Bu_3SnH over 60−70 min. After 60 min of reflux, the solution was cooled, CCl_4 (10 mL) was added, and the mixture stirred for 20 min. A solution of iodine in dichloromethane was added to the above solution until a faint coloration persisted, and then solvent was evaporated. The solid so obtained was taken up in ethyl acetate and repeatedly washed with saturated aqueous solution of potassium fluoride till white flocculent precipitate was seen. The organic layer was dried evaporated and chromatographed over silica gel (10−60% ethyl acetate in cyclohexane, v/v) to give a diastereomeric mixture **11a/11b** in 73% yield (1.6 g, 3.5 mmol). $R_f = 0.40$ (30% ethyl acetate in cyclohexane, v/v). ^{13}C NMR (125.7 MHz) δ: 163.8, 149.7, 137.7, 137.4, 136.3, 136.2, 128.5, 128.4, 128.3, 127.8, 127.8, 127.7, 127.7, 127.6, 127.4, 109.0, 88.8, 88.6, 84.1, 78.6, 78.1, 77.1, 73.6, 71.9, 71.7, 67.5, 67.4, 47.9, 47.8, 38.6, 37.6, 33.5, 28.7, 20.0, 15.4, 12.0, 11.9; MALDI-TOF m/z $[M + H]^+$ found 463.11 calcd 463.22.

(1*R*,3*R*,4*R*,5*R*,7*S*)-7-Hydroxy-1-hydroxymethyl-3-(thymin-1-yl)-2-oxa-bicyclo[2.2.1]heptane (12). To a solution of **11a/11b (**1.5 g, 3.24mmol) in dry methanol were added 20% $Pd(OH)_2$/C (1.6 g) and ammonium formate (4.0 g, 65 mmol) and refluxed. The same amount of ammonium formate and 20% $Pd(OH)_2$/C was added twice after 3 h and the reaction refluxed for 8 h. After the reaction was finished as seen by TLC, the suspension was filtered over celite and organic phase evaporated and chromatographed over silica gel (2−7% methanol in dichloromethane, v/v) to obtain **12a/12b (**0.70 g, 2.4mmol, 76%) as a white powder. $R_f = 0.50$ (7% methanol in dichloromethane, v/v). ^{1}H NMR (600 MHz, D_2O) of **12a** δ: 7.81 (1H, s, H6, thymine), 5.78 (1H, s, H1′), 4.18 (1H, d, 4.4 Hz, H3′), 3.85 (1H, d, $J_{H5',5''} = 12.6$ Hz, H5′), 3.83 (1 H, d, $J_{H5',5''} = 12.6$ Hz, H5″), 2.65 (1H, m, H7′), 2.43 (1H, d, $J_{H2',H7'} = 4.4$ Hz, H2′), 2.04 (1H, dd, $J_{H6',H6''} = 12.3$ Hz, $J_{H7',H6''} = 10.6$ Hz, H6″), 1.89 (3H, d, $J = 1.25$ Hz, thymine CH_3), 1.23 (3H, d, $J_{H7',CH3} = 7.3$ Hz, C7′-CH_3), 1.17 (1H, dd, $J_{H6',H6''} = 12.3$ Hz, $J_{H7',H6''} = 4.9$ Hz, H6′); ^{13}C NMR (125.7 MHz, D_2O) δ: 166.64 (C4), 151.05 (C2), 137.33 (C6), 109.7 (C5), 90.6 (C4′), 83.7 (C1′), 71.7 (C3′), 58.7 (C5′), 49.7 (C7′), 36.0, (C6′), 28.1 (C7′), 14.4 (C7′-methyl) 11.5 (thymine CH_3); MALDI-TOF m/z $[M + H]^+$ found 283.94, calcd 283.14.

(1*R*,3*R*,4*R*,5*R*,7*S*)-7-Hydroxy-1-(4,4′-dimethoxytrityloxymethyl)-3-(thymin-1-yl)-2-oxa-bicyclo[2.2.1]heptane (13). Compound **12** (0.70 g, 2.4 mmol) was evaporated twice with dry pyridine and suspended in the same. 4,4′-Dimethoxytrityl chloride (1.26 g, 3.7 mmol) was added and stirred overnight. Reaction was quenched with saturated aqueous $NaHCO_3$ and extracted thrice with dichloromethane (50 mL). The organic phase was dried, evaporated, and chromatographed over silica gel (1% pyridine/ethyl acetate in cyclohexane, v/v) to give **13** (1.0 g, 1.8 mmol, 74%) as yellow foam. R_f = 0.60 (5% methanol in dichloromethane, v/v). ^{1}H NMR (600 MHz) δ: 8.52 (NH thymine), 7.81 (1H, s, H6 thymine), 6.88−7.34 (13H, m), 5.78 (1H, s, H1′), 4.31 (1H, s, H3′), 3.66 (1H, d, $J_{H5',H5''}$ = 12.6 Hz, H5″), 3.55 (1H, d, $J_{H5',H5''}$ = 12.6 Hz, H8′), 2.65 (1H, m, H7′), 2.4 (1H, d, $J_{H2',H3''}$ = 4.4 Hz, H2′), 2.04 (1H, dd, $J_{H6',H6''}$ = 12.3 Hz, $J_{H7',H6''}$ = 10.6 Hz, H6″), 1.89 (3H, d, J = 1.3 Hz, thymine CH_3), 1.23 (3H, d, 7.3 Hz, CH_3-C7′), 1.17 (1H, dd, $J_{H6',H6''}$ = 12.3 Hz, $J_{H6',H7'}$ = 4.9 Hz, H6′); ^{13}C NMR (600 MHz, D_2O) δ: 164 (C4), 158.7, 149. 8 (C2), 135.6, 135.7, 135.9 (aromatic), 130 (C6), 113.3, 127.1, 128, 128.1 (aromatic), 109.4 (C5), 89.4 (C4′), 84.1 (C1′), 73.1 (C3′), 61 (C5′), 55.2 (OCH_3), 50.4 (C2′), 37.4 (C6′), 28.5 (C7′), 15.3 (C7′-methyl), 12.3 (CH_3, thymine); MALDI-TOF m/z $[M + H]^+$ found 585.22, calcd 585.25.

(1*R*,3*R*,4*R*,5*R*,7*S*)-7-(2-(Cyanoethoxy-(diisopropylamino)-phosphinoxy)-1-(4,4′-dimethoxytrityloxymethyl)-3-(thymin-1-yl)-2-oxa-bicyclo[2.2.1]heptane (14). Compound **13** (0.5 g, 0.85 mmol) was dissolved in 6 mL of dry THF, DIPEA (0.57 mL, 0.2 mmol) was added at 0 °C followed by 2-cyanoethyl *N*,*N*-diisopropyl phosphoramidochloridite (0.4 mL, 1.7 mmol), and reaction was stirred overnight at room temperature. Methanol (0.5 mL) was added followed by aqueous saturated $NaHCO_3$ and extracted twice (25 mL) with dichloromethane. The organic phase was dried, evaporated, and chromatographed on silica gel (1% Et_3N, ethyl acetate in cyclohexane, v/v) to give **14** (0.5 g, 80%) as a mixture of four isomers; ^{31}P NMR (109.4 MHz, $CDCl_3$): 148.82, 149.19, 149.36, 150.08. The four signals in ^{31}P NMR have been integrated and are found to be in the ratio of 7:3 as found in the ^{1}H NMR spectrum of **12a**/**12b**. The integration is included in the SI (Inset in Figure S42). MALDI-TOF m/z $[M + H]^+$ found 785.67, calcd 785.36.

3,5-Di-*O*-benzyl-4-*C*-hydroxypropyl-1,2-*O*-isopropylidene-α-D-ribofuranose (15). A 0.5 M solution of 9-BBN (88 mL, 44 mmol) was added dropwise to a solution of **6** (6 g, 14 mmol) in dry THF (100 mL) and stirred overnight. Water was added till gas evolution stopped, 3 N NaOH solution (25 mL) was then added, and slowly 33% aqueous H_2O_2 was added while the temperature was maintained at not more than 50 °C. The mixture was stirred for about 30 min at room temperature, partitioned between ethyl acetate and water, and extracted twice with ethyl acetate (100 mL). The organic layer was dried, evaporated, and purified over silica gel (30−35% ethyl acetate in cyclohexane, v/v) to give **15** as a colorless oil (5.4 g, 13 mmol, 90%); R_f = 0.40 (50% ethyl acetate in cyclohexane, v/v). ^{1}H NMR (270 MHz $CDCl_3$) δ: 7.32 (10H, m, benzyl) 5.75 (1H, $J_{H1,H2}$ = 4 Hz, H1) 4.76 (1H, d, J_{gem} = 12.1 Hz, CH_2Bn), 4.62 (1H, app t, 4.6 Hz, H2), 4.6 (1H, d, J_{gem} = 12.3 Hz, CH_2Bn), 4.52 (1H, d, J_{gem} = 12.3 Hz, CH_2-Bn), 4.52 (1H, d, J_{gem} = 12 Hz, CH_2Bn) 4.41 (1H, d, J_{gem} = 12 Hz, CH_2Bn), 4.15 (1H, d, J = 5.3 Hz, H3), 3.83 (2H, m, H8,8′) 3.49 (1H, d, $J_{H5',H5''}$ = 10.3 Hz, H5′), 3.3 (1H, d, $J_{H5',H5''}$ = 10.3 Hz, H5″), 2.95 (2H, m, H6′, H7′) 1.72 (2H, m, H6″,7″), 1.60 (3H, CH_3), 1.31 (3H, CH_3); ^{13}C NMR (67.9 MHz) δ: 138.1, 128.4, 127.9, 127.7, 127.6, 113.1 (aromatic), 104.1 (C1), 87.1 (C4), 79.1 (C2), 78.6 (C3), 73.5 (CH_2-Bn), 72.5 (CH_2Bn), 72.4 (C5), 62.7 (C8), 27.8 (C7), 26.9 (C6), 26.5 (CH_3), 26.0 (CH_3); MALDI TOF m/z $[M + Na]^+$ found 451.12, calcd 451.2.

3,5-Di-*O*-benzyl-4-*C*-penten-yl-1,2-*O*-isopropylidene-α-D-ribofuranose (17). Oxalyl chloride (2.48 mL, 29.20 mmol) was added to dichloromethane (100 mL) and cooled at −78 °C. DMSO (3.3 mL, 46.72 mmol) was added dropwise to this solution over 30 min. After stirring for an additional 20 min, a solution of **2** (5 g, 11.68 mmol) in dichloromethane (50 mL) was added dropwise to this mixture over 20 min and stirred at −78 °C for another 45 min. DIPEA (13 mL, 100 mmol) was added to this cooled mixture and allowed to warm to room temperature. Water was added to the reaction and twice extracted with dichloromethane (100 mL). The organic layer was washed with water and brine, dried over $MgSO_4$, and concentrated under reduced pressure. In another reaction BuLi (1.6 M solution in hexane, 22 mL, 35 mmol) was added to a precooled suspension of methyl-triphenylphosphonium bromide (12.5 g, 35 mmol) at 0 °C in dry THF and stirred at room temperature for 1 h. The yellow solution so obtained was cooled to −78 °C, and a solution of crude aldehyde in dry THF was then added dropwise over 20 min and stirred at −78 °C overnight. The reaction was quenched with saturated aqueous NH_4Cl, stirred for about 1 h at room temperature, extracted with ether (3 × 100 mL), dried over $MgSO_4$, and concentrated under reduced pressure. The crude material was purified by column chromatography on silica gel (0−10% ethyl acetate in cyclohexane, v/v) to give **17** as a yellowish oil (3.5 g, 8.4 mmol, 72%). R_f = 0.40 (30% ethyl acetate in cyclohexane, v/v). ^{1}H NMR (270 MHz, $CDCl_3$) δ: 7.35 (10H, m), 5.84 (1H, m, H8), 5.76 (1H, d, $J_{H1,H2}$ = 4 Hz, H1), 4.95 (2H, m, H9, 9′), 4.80 (1H, d, J_{gem} = 12.1 Hz, CH_2Bn), 4.62 (1H, app t, J = 4.5 Hz, H2), 4.60 (1H, d, J_{gem} = 12.1 Hz, CH_2Bn), 4.53 (1H, d, J_{gem}= 11.9 Hz, CH_2Bn), 4.4 (1H, d, J_{gem} = 12 Hz, CH_2Bn), 4.15 (1H, d, $J_{H2,H3}$ = 5.2 Hz, H3), 3.51 (1H, d, $J_{H5,H5'}$ = 10.3 Hz, H5), 3.31 (1H, d, $J_{H5,H5'}$ = 10.3 Hz, H5′), 2.35 (2H, m, H6 and H6′), 2.1 (1H, m, H7′), 1.70 (1H, m, H7′), 1.62 (3H, s, CH_3), 1.33 (3H, s, CH_3); ^{13}C NMR (67.9 MHz) δ: 139.1 (C8), 138.2, 128.4, 127.8, 127.7 (aromatic), 114.2 (C9), 113.1, 104.1 (C1), 86.7 (C4), 79.3 (C2), 78.7(C3), 73.5 (CH_2Bn), 72.8 (C5), 72.4 (CH_2Bn) 30.9 (C7), 27.8 (C6), 26.70 (CH_3), 26.3 (CH_3).

1-[3,5-Di-*O*-benzyl-4-*C*-penten-yl-2-hydroxy-β-D-ribofuranosyl]-thymine (20). Acetic anhydride (9.5 mL, 50 mmol) and acetic acid (50 mL) were added to **4** (3.5 g, 8.2 mmol) and cooled on ice bath, and triflic acid (0.03 mL, 0.4 mmol) was added to it and stirred. After 30 min, the reaction was quenched with cold saturated $NaHCO_3$ solution and extracted with dichloromethane. The organic layer was dried and evaporated. The crude product was coevaporated with dry CH_3CN thrice and dissolved in the same. Thymine (1.5 g, 12.37 mmol) and *N*,*O*-bis-(trimethylsilyl)acetamide (5.0 mL, 24.75 mmol) were added to this solution and refluxed for 45 min till the suspension became a clear solution. This solution was cooled to 0 °C, and TMSOTf (1.71 mL, 9.9 mmol) was added dropwise and stirred overnight. The reaction was quenched with saturated NH_4Cl solution and extracted with dichloromethane. The organic layer was dried, evaporated, and treated with 27% methanolic ammonia overnight. After completion of the reaction, the solvent was evaporated and the residue purified over silica gel (0−3% methanol in dichloromethane, v/v) to give **21** as a white foam (2.8 g, 5.77 mmol, 70% in three steps). R_f = 0.50 (5% methanol in dichloromethane, v/v). ^{1}H NMR (270 MHz, $CDCl_3$) δ: 7.51 (1H, s, H-6), 7.3 (10H, m, benzyl), 6.00 (1H, d, $J_{H1',H2'}$ = 5.44 Hz, H1′), 5.76 (1H, m, H8′), 4.94 (2H, m, H9′ and H9″), 4.84 (1H, d, J_{gem} = 11.8 Hz, CH_2Bn), 4.58 (1H, d, J_{gem} = 11.8 Hz, CH_2Bn), 4.52 (1H, d, J_{gem} = 12 Hz, CH_2Bn), 4.48 (1H, d, J_{gem} = 12 Hz, CH_2Bn), 4.41 (1H, app t, J = 5.6 Hz, H2′), 4.15 (1H, d, $J_{H2',H3'}$ = 5.8 Hz, H3′), 3.69 (1H, d, $J_{H5',H5''}$ = 9.9 Hz, H5″), 3.41 (1H, d, $J_{H5',H5''}$ = 9.9 Hz, H5′), 2.22 (1H, m, H6′), 2.04 (2H, m, H7′ and H7″), 1.63 (1H, m, H6′), 1.49 (3H, thymine CH_3); ^{13}C NMR (67.9 MHz, $CDCl_3$) δ: 164.2 (C2), 151.4 (C4), 138.5 (C8′), 136 (C6), 137.4, 130.0, 128.7, 128.5, 128.1, 127.7 (aromatic), 114.6 (C9′), 111.0 (C5), 88.8 (C1′), 87.3 (C4′), 79.1 (C3′), 75.1 (C2′), 73.3 (C5′), 73.6 (CH_2Bn), 73.4 (CH_2Bn), 31.9 (C6′), 27.7 (C7′), 12.1 (CH_3, thymine); MALDI-TOF m/z $[M + H]^+$ found 493.11, calcd 493.17.

1-[3,5-Di-*O*-benzyl-4-*C*-penten-yl-2-*O*-phenoxythiocarbonyl-β-D-ribofuranosyl]-thymine (21). The nucleoside **20** (2.8 g, 5.7mmol) was evaporated thrice with dry pyridine and dissolved in the same. To this precooled solution was added DMAP (0.69 g, 5.7 mmol), dropwise was added phenyl chlorothionoformate (1.15 mL, 8.55 mmol), and the

reaction was stirred overnight. The reaction was quenched with saturated solution of $NaHCO_3$ and extracted with dichloromethane. Organic layer was dried over $MgSO_4$, concentrated, and chromatographed over silica gel (10−30% ethyl acetate in cyclohexane, v/v) to give **21** as a yellowish foam (2.1 g, 3.42 mmol, 60%). $R_f = 0.60$ (30% ethyl acetate in cyclohexane, v/v). ^{1}H NMR (600 MHz, $CDCl_3$) δ: 8.32 (1H, br s, NH), 7.48 (1H, s, H6), 7.48−6.99 (15H, m), 6.4 (1H, d, $J_{H1',H2'} = 6.3$ Hz, H1′), 5.94 (1H, app t, $J = 6.0$ Hz, H2′), 5.77 (1H, m, H8′), 4.97 (2H, m, H9′ and H9″), 4.77(1H, d, J_{gem}= 12 Hz, CH_2Bn), 4.55 (3H, d, $J_{gem} = 12$ Hz, CH_2Bn), 4.53 (1H, d, $J_{H2',H3'} = 5.8$ Hz, H3′), 3.74 (1H, d, $J_{H5',H5''} = 9.9$ Hz, H5″), 3.47 (1H, d, $J_{H5',H5''} = 9.9$ Hz, H5′), 2.22 (1H, m, H7′), 2.06 (1H, m, H7″), 1.94 (1H, m, H6′), 1.66 (1H, m, H6″), 1.53 (3H, thymine CH_3); ^{13}C NMR (125.7 MHz, $CDCl_3$) δ: 194.4 (C═S), 163.3 (C4), 153.3, 150.2 (C2), 138.1 (C8′), 137.3, 137.0, 135.6 (C6), 129.5−121.9 (aromatic), 114.8 (C9′), 111.5 (C5), 87.6 (C4′), 85.1 (C1′), 82.9 (C2′), 78.1 (C3′), 74.9 (CH_2Bn), 73.7 (C5′), 73.6 (CH_2Bn), 31.6 (C6′), 27.6 (C7′), 12.0 (CH_3 thymine); MALDI-TOF *m*/*z* [M + H]$^+$ found 629.09, calcd 629.73.

(1*R*,2*R*,5*R*,7*R*,8*S*)-8-Benzyloxy-5-benzyloxymethyl-7-(thymin-1-yl)-6-oxa-bicyclo[3.2.1]octane (22). 21 (2.1 g, 3.3 mmol) was dissolved in 200 mL of dry toluene, purged for 30 min, and then refluxed. Bu_3-SnH (0.8 mL, 3.0 mmol) dissolved in 25 mL of dry toluene was added dropwise to this solution and refluxed for 15 min. AIBN (0.768 g, 4mmol) was dissolved in dry toluene and added dropwise to the refluxing solution over 60 min. Simultaneously was added Bu_3SnH (0.8 mL, 3.3 mmol) dissolved in 25 mL of dry toluene, and the reaction was refluxed till starting material was exhausted in about an additional 60 min. The reaction was cooled, and 25 mL of CCL_4 was added followed by addition of a solution of iodine dissolved in ether till the color persisted. The solvent was evaporated over vacuum and the residue taken up in diethyl ether and repeatedly washed with a saturated solution of potassium fluoride. The ether layer was dried, evaporated, and chromatographed over silica gel (0−20% ethyl acetate in cyclohexane, v/v) to give **22** as a white powder (1.19 g, 2.5 mmol, 76%). $R_f = 0.40$ (30% ethyl acetate in cyclohexane, v/v). ^{1}H NMR (600 MHz, $CDCl_3$) δ: 8.71 (1H, br s, NH), 8.06 (1H, s, H6), 7.3 (10H, m), 5.82 (1H, s, H1′), 4.56 (2H, dd, $J_{gem} = 10.8$ Hz, CH_2Bn), 4.54 (1H, d, $J_{gem} = 10.8$ Hz, CH_2Bn), 4.47(1H, d, $J_{gem} = 10.8$ Hz, CH_2Bn), 4.17 (1H, d, $J_{H2',H3'} = 5.4$ Hz, H3′), 3.69 (1H, d, $J_{H5',H5''} = 10.8$ Hz, H5′), 3.55 (1H, d, $J_{H5',H5''} = 10.8$ Hz, H5″), 2.31 (1H, d, $J_{H2',H3'} = 4.8$ Hz, H2′), 2.22 (1H, m, H8′), 1.83 (1H, m, H7′), 1.66 (1H, m, H6″), 1.43 (3H, s, CH_3 thymine), 1.33 (2H, m, H6′, H7″), 1.11 (3H, $J_{CH3,H8'} = 7.2$ Hz, CH_3-C8′); ^{13}C NMR (125.7 MHz, $CDCl_3$) δ: 164.1 (C4), 149.9 (C2) 137.4, 136.6 (C6), 128.5, 128.3, 128.0, 127.8, 127.3, 109.1(C5), 84.7 (C1′), 84.6 (C4′), 73.5(C3′), 73.51 (CH_2Bn), 71.7 (CH_2Bn), 70.6 (C5′), 48.4 (C2′), 27.0 (C6′), 26.5 (C7′), 25.6 (C8′), 18.9(C8′, methyl), 11.8 (CH_3, thymine); MALDI-TOF *m*/*z* [M + H]$^+$ found 477.56, calcd 477.39.

(1*R*,2*R*,5*R*,7*R*,8*S*)-8-Hydroxy-5-hydroxymethyl-7-(thymin-1-yl)-6-oxa-bicyclo[3.2.1]octane (23). Compound **22** (1.2 g, 2.5 mmol) was dissolved in dry methanol. 20% $Pd(OH)_2$/C (1.3 g) and ammonium formate (3.4 g, 50 mmol) were added and refluxed. The same amount of ammonium formate and 20% $Pd(OH)_2$/C was added thrice after every 3 h, and the reaction was refluxed overnight. After the reaction was finished as seen by TLC, the suspension was filtered over celite and the organic phase evaporated and chromatographed over silica gel (2−7% methanol in dichloromethane, v/v) to give **25** as a white powder (0.60 g, 2.0 mmol, 82%). $R_f = 0.50$ (10% methanol in dichloromethane, v/v). ^{1}H NMR (600 MHz, D_2O) δ: 8.19 (1H, s, H6), 5.77 (1H, s, H1′), 4.25 (1H, d, $J_{H2',H3'} = 5.2$ Hz, H3′), 3.71 (2H, s, H5′ and H5″), 2.26 (1H, d, $J_{H2',H3'} = 5.2$ Hz, H2′), 2.20 (1H, m, H8′), 1.86 (3H, s, CH_3-thymine), 1.68 (1H, m, H6′), 1.36 (1H, m, H7′), 1.25 (2H, m, H7″, H6″), 1.05 (3H, d, $J_{CH3,H8'} = 7$ Hz, C8′-CH_3); ^{13}C NMR (125.7 MHz, $CDCl_3$) δ: 165.0 (C4), 150.8 (C2), 137.4 (C6), 108.0 (C5), 86.0 (C4′), 84.2 (C1′), 65.5 (C3′), 62.3 (C5′), 51.6 (C2′), 27.3 (C6′), 26.6 (C7′), 25.5 (C8′), 19.9 (C8′-CH_3), 13.3 (CH_3, thymine); MALDI-TOF *m*/*z* [M]$^+$ found 296.97, calcd 296.14.

(1*R*,2*R*,5*R*,7*R*,8*S*)-5-(4,4′-Dimethoxytrityloxymethyl)-8-hydroxy-7-(thymin-1-yl)-6-oxa-bicyclo[3.2.1]octane (24). Compound **23** (0.5 g, 1.68 mmol) was evaporated twice with dry pyridine and then suspended in the same. 4,4′-dimethoxytrityl chloride was added and stirred at room temperature overnight. Reaction was quenched with aqueous $NaHCO_3$ and extracted with dichloromethane. The organic layer was dried, evaporated, and chromatographed on silica gel (1% pyridine, ethyl acetate in cyclohexane, v/v) to give **26** (0.8 g, 1.34 mmol, 80%) as a yellowish foam. $R_f = 0.60$ (30% ethyl acetate in cyclohexane, v/v). ^{1}H NMR (600 MHz, $CDCl_3$ + DABCO) δ: 7.8 (1H, s, H6), 6.83−7.4 (13 H, m), 5.77 (1H, s, H1′), 4.44 (1H, d, $J_{H2',H3'} = 5.2$ Hz, H3′), 3.78 (6H, s, 2× OCH_3), 3.36 (1H, d, $J_{H5',H5''} = 10.6$ Hz, H5′), 3.26 (1H, d, $J_{H5',H5''} = 10.6$ Hz, H5″), 2.30 (1H, m, H8′), 2.27 (1H, d, $J_{H2',H3'} = 5.2$ Hz, H2′), 1.77 (1H, m, H6″), 1.64 (1H, m, H7′), 1.36 (1H, m, H7″), 1.25 (2H, m, H6′ and H7′), 1.1 (3H, d, $J_{H8',CH3} = 7$ Hz, C8′-CH_3); ^{13}C NMR (125.7 MHz) δ: 164.1 (C4), 158.6 (C2), 158.6, 149.9, 144.3, 135.9 (C6), 135.4, 135.3, 130.0, 128.1, 128.0, 127.1, 113.2, 109.4, 84.8 (C1′), 84.8 (C4′), 67.9 (C3′), 54.5 (C5′), 55.2 (OCH_3), 50.8 (C2′), 46.9 (DABCO), 26.9 (C7′), 26.4 (C6′), 25.0 (C8′), 18.9 (C8′-CH_3), 11.9 (CH_3, thymine); MALDI-TOF *m*/*z* [M + Na]$^+$ found 621.59, calcd 621.29.

(1*R*,2*R*,5*R*,7*R*,8*S*)-8-(2-(Cyanoethoxy(diisopropylamino)-phosphinoxy)-5-(4,4′-dimethoxytrityloxymethyl)-7-(thymin-1-yl)-6-oxa-bicyclo-[3.2.1]octane (25). Compound **24** (0.5 g, 0.83 mmol**)** was dissolved in 6 mL of dry THF, diisopropylethylamine (0.75 mL, 4.18 mmol) was added, and the reaction was cooled in an ice bath. To this was added 2-cynoethyl *N*,*N*-diisopropylphosphoramidochloridite (0.36 mL, 1.66 mmol), and the mixture was stirred overnight at room temperature. Reaction was quenched by addition of cold aqueous $NaHCO_3$ and extracted with dichloromethane. The organic layer was dried, evaporated, and chromatographed over silica gel (1% Et_3N, ethyl acetate in cyclohexane, v/v) to give **27** (0.55 g, 0.7 mmol 84%); ^{31}P NMR (109.4 MHz, $CDCl_3$) δ 149.25, 150.26; MALDI-TOF *m*/*z* [M + H]$^+$ found 799.64, calcd 799.9.

UV Melting Experiments. All 17 modified AONs have been purified as a single component on PAGE (20% polyacrylamide with 7 M urea), extracted with 0.3 M NaOAc, and desalted with a C-18 reverse phase cartridge to give AONs in >99% purity, and correct masses have been obtained by MALDI-TOF mass spectroscopy for each one of them (Table 1). Determination of the T_m of the AON/RNA hybrids was carried out in the following buffer: 57 mM Tris-HCl (pH 7.5), 57 mM KCl, 1 mM $MgCl_2$. Absorbance was monitored at 260 nm in the temperature range from 20 °C to 90 °C using an UV spectrophotometer equipped with a Peltier temperature programmer with the heating rate of 1 °C per minute. Prior to measurements, the samples (1 μM of AON and 1 μM RNA mixture) were preannealed by heating to 90 °C for 5 min followed by slow cooling to 4 °C and 30 min equilibration at this temperature. and are the average of at least three independent runs.

^{32}P Labeling of Oligonucleotides. The oligoribonucleotides and oligodeoxyribonucleotides were 5′-end labeled with ^{32}P using T4 polynucleotide kinase, [γ-^{32}P]ATP, and the standard protocol.[71] Labeled AONs and the target RNA were purified by 20% denaturing PAGE, and specific activities were measured using a Beckman LS 3801 counter.

Exonuclease Degradation Studies. Stability of the AONs toward 3′-exonucleases was tested using snake venom phosphodiesterase (SVPDE) from *Crotalus adamanteus*. All reactions were performed at 3 μM DNA concentration (5′-end ^{32}P labeled with specific activity 80 000 cpm) in 56 mM Tris-HCl (pH 7.9) and 4.4 mM $MgCl_2$ at 21 °C. An exonuclease concentration of 17.5 ng/μL was used for digestion of oligonucleotides. Total reaction volume was 14 μL. Aliquots were taken at 1, 2, 24, 48, and 72 h and quenched by addition of the same volume of 50 mM EDTA in 95% formamide. Reaction progress was monitored by 20% denaturing (7 M urea) PAGE and autoradiography.

Stability Studies in Human Serum. AONs (6 μL) at 2 μM concentration (5′-end ^{32}P labeled with specific activity 80 000 cpm)

were incubated in 26 μL of human blood serum (male AB) at 21 °C (total reaction volume was 36 μL), and the experiments were repeated twice up to 48 h. Aliquots (3 μL) were taken at 0, 30 min, 1, 2, 5, 7, 8, 9, 12, 24, 36, 48 h, and quenched with 7 μL of solution containing 8 M urea and 50 mM EDTA, resolved in 20% polyacrylamide denaturing (7 M urea) gel electrophoresis and visualized by autoradiography. The ^{32}P label at the 5′-terminus was cleaved gradually by the phosphatases present in the blood serum, which resulted in a lower radioactive count as the digestion progressed with time. Since no new prominent cleavage products were found toward the later time points, we considered those prominent stable initial fragments as 100% during the last time points (12−48 h).

Theoretical Calculations. Carbocyclic analogues of the ENA and LNA nucleosides have been investigated *in silico* using *ab initio* and molecular dynamics techniques. Their molecular structures have been refined using Amber force field and available structural information from NMR experiments according to the following protocol: (i) Derive initial dihedral angles from the observed $^3J_{H,H}$ using Haasnoot−de Leeuw−Altona generalized Karplus equation;[66,67] (ii) perform NMR-constrained molecular dynamics (MD) simulation (0.5 ns, 10 steps) and simulated annealing (SA) followed by 0.5 ns NMR-constrained simulations at 298 K using the NMR-derived torsional constraints from Step i to yield NMR-defined molecular structures; (iii) acquire 6-31G** Hartree−Fock optimized *ab initio* gas-phase geometries in order to compare the experimentally derived torsions with the *ab initio* geometry; (iv) analyze the full conformational hyperspace using 2 ns NMR/*ab initio*-constrained MD simulations of compounds **12a**, **12b**, and **23** followed by full relaxation of the constraints.

The geometry optimizations of the modified nucleosides have been carried out by GAUSSIAN 98 program package[86] at the Hartree−Fock level using 6-31G** basis set. The atomic charges and optimized geometries of compounds **12a**, **12b**, and **23** were then used as AMBER[87] force field parameters employed in the MD simulations. The protocol of the MD simulations is based on Cheathan−Kollman's[88] procedure employing a modified version of Amber 1994 force field as it is implemented in AMBER 7 program package.[87] Periodic boxes containing 718 (**12a**, **12b**) and 753 (**23**) TIP3P[89] water molecules, to model explicit solvent around the compounds, were generated using xleap extending 12.0 Å from these molecules in three dimensions in both the NMR-constrained and -unconstrained MD simulations. The SA protocol included ten repeats of 25 ps heating steps from 298 to 400 K followed by fast 25 ps cooling steps from 400 to 298 K. During these SA and NMR-constrained MD simulations, torsional constraints of 50 kcal mol^{-1} rad^{-2} were applied. The constraints were derived from the experimental $^3J_{H2',H3'}$ and available $^3J_{H2',H7'/H8}$ coupling constants using Haasnoot−de Leeuw−Altona generalized Karplus equation.[66,67] Ten SA repeats were followed by 0.5 ns MD run at a constant 298 K temperature applying the same NMR constraints.

Generalized Karplus Parametrization. Relevant vicinal proton $^3J_{H,H}$ coupling constants have been back-calculated from the corresponding theoretical torsions employing Haasnoot−de Leeuw−Altona generalized Karplus equation[66,67] taking into account β substituent correction in form:

$$^3J = P_1 \cos^2(\phi) + P_2 \cos(\phi) + P_3 + \sum (\Delta\chi_i^{\text{group}} (P_4 + P_5 \cos^2(\xi_i \phi + P_6 |\Delta\chi_i^{\text{group}}|))$$

where $P_1 = 13.70$, $P_2 = -0.73$, $P_3 = 0.00$, $P_4 = 0.56$, $P_5 = -2.47$, $P_6 = 16.90$, $P_7 = 0.14$ (parameters from ref 66), and $\chi_i^{\text{group}} = \Delta\chi_i^{\alpha-\text{substituent}} - P_7 \sum \Delta\chi_i^{\beta-\text{substituent}}$ where $\Delta\chi_i$ are taken as Huggins electronegativities.[90]

Acknowledgment. Generous financial support from the Swedish Natural Science Research Council (Vetenskapsrådet), the Swedish Foundation for Strategic Research (Stiftelsen för Strategisk Forskning), and the EU-FP6 funded RIGHT project (Project no. LSHB-CT-2004-005276) is gratefully acknowledged. We would like to thank Mr. O.P. Varghese for providing aza-ENA-T modified AONs for this study. Puneet Srivstava (P.S.) has planned and carried through total synthesis of carbocyclic nucleosides, their incorporations into oligos, enzymology, physicochemical studies, and NMR characterization. Małgorzata Wenska was responsible for the scale-up of compound **23** using P.S.'s procedure. Jharna Barman has performed enzymological experiments with P.S. Wimal Pathmasiri has performed detailed NMR characterization by 500/600 MHz NMR and simulation. Oleksandr Plashkevych has performed molecular structure analysis based on the NMR experiments and *ab initio* and MD simulations.

Supporting Information Available: ^{1}H and ^{13}C NMR spectra of compounds **2**−**17** and **20**−**24**; ^{31}P NMR of compounds **14** and **25**; 1D NOE of **12a**/**12b** and **23**; DEPT spectra of compounds **12a**/**12b** and **23**; COSY spectra of **12a**/**12b** and **23**; TOCSY spectra of **12a**/**12b** and **23**; HMQC spectra of **10**, **11a**/**11b**, **12a**/**12b**, **21**, **22**, and **23**; HMBC spectra of **10**, **11a**/**11b**, **12a**/**12b**, **21**, **22**, and **23**; $^3J_{HH}$ simulations of compounds **12a**/**12b** and **23**; plots of percentage remaining of AONs **6**−**17** in human blood serum with time; SVPDE digestion profile of AONs **1**−**17** (denaturing PAGE autoradiograms); plots of percentage remaining of AONs **6**−**17** in SVPDE; correlation of experimental $^3J_{H1',H2'}$ and $^3J_{H2',H3'}$ vicinal coupling constants in carbocyclic-ENA-T (**12a**,**12b**) and carbocyclic LNA-T (**23**) as well as their 2′-O- and 2′-N-analogues (ENA-T, aza-ENA-T, LNA-T, and 2′-amino-LNA-T); overlay of 2500 molecular structures of the carbocyclic-ENA-T nucleoside collected every 0.2 ps of the last 500 ps (1.5−2.0 ns) of its MD simulation and their analysis; tables of ^{1}H chemical shifts and $^3J_{HH}$ coupling constants for compounds **11**, **12a**/**12b**, **22**, and **23**; table of experimental and theoretical $^3J_{HH}$ vicinal coupling constants and tables of sugar torsions, pseudorotational phase angle, sugar puckering amplitude, and solvation energy (E_{solv}) calculated using Baron and Cossi's implementation of the polarizable conductor CPCM model;[85] and a complete discussion of structure assignment of bicyclic system for compounds **12a**/**12b** and **23** as well as their molecular structures based on NMR, *ab initio*, and MD calculations. This material is available free of charge via the Internet at http://pubs.acs.org.

JA071106Y

(86) Frisch, M. J., et al. *Gaussian 98 (Revision A.6)*. Gaussian, Inc.: Pittsburgh, PA, 1998.
(87) Case, D. A., et al. *AMBER 7*. University of California: San Francisco, 2002.
(88) Cheatham, T. E., III; Kollman, P. A. *J. Am. Chem. Soc.* **1997**, *119*, 4805−4825.
(89) Jorgensen, W. L.; Chandrasekhar, J.; Madura, J. D.; Impey, R. W.; Klein, M. L. *J. Chem. Phys.* **1983**, *79*, 926−935.
(90) Huggins, M. L. *J. Am. Chem. Soc.* **1953**, *75*, 4123−4126.